

Hybrid Synthetic and Computational Study of an Optimized, Solvent-Free Approach to Curcuminoids

Valeria A. Stepanova,* Andres Guerrero,¹ Cullen Schull,¹ Joshua Christensen, Claire Trudeau, Joshua Cook, Kyle Wolmutt, Jordan Blochwitz, Abdelrahman Ismail, Joseph K. West, Amelia M. Wheaton, Ilia A. Guzei, Bin Yao, and Alena Kubatova



Cite This: *ACS Omega* 2022, 7, 7257–7277



Read Online

ACCESS |



Metrics & More

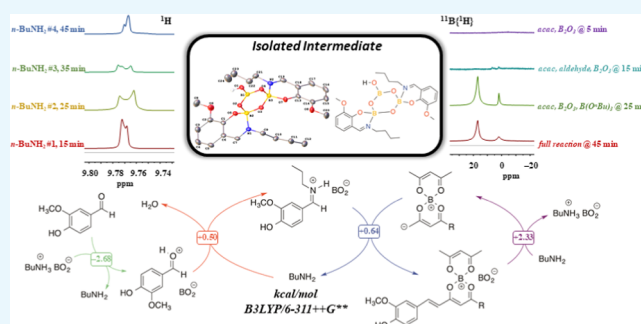


Article Recommendations



Supporting Information

ABSTRACT: A green and optimized protocol has been developed for the preparation of symmetric 1,7-bis(aryl)-1,6-heptadiene-3,5-diones and asymmetric 2-aryl-6-arylidencyclohexanones with modified substrate scope and good functional group tolerance. Syntheses proceed smoothly under solvent-free conditions, providing moderate to excellent product yields with a minimal workup procedure. Control experiments, spectroscopic, and computational studies support a mechanism involving the boron-assisted in situ generation of imine intermediates. Crystal structures of three curcuminoids and isolated mechanistic intermediates are reported. The data provide insight for the further development of solvent-free protocols toward diverse curcumin derivatives in the fields of pharmaceutical and synthetic chemistries.



INTRODUCTION

Since the discovery of curcumin and its wide range of biological properties, it has become one of the most cited naturally occurring molecules.¹ In this work, the development of a solvent-free curcumin and curcuminoid synthesis protocol and the study of the underlying mechanism using a combination of synthetic, spectroscopic, and computational methods are described. A wide range of bioactivities of curcumin are described in detail elsewhere.^{1,2}

The vast majority of curcumin is extracted from rhizomes of the *Curcuma longa* (Turmeric) plant also known as *kunir* (Javanese) or *kunyit* (Indonesian).¹ The global market of curcumin was estimated at USD 58.4 million in 2019 and is expected to experience a compound annual growth rate (CAGR) of 12.7% by 2024.³ The active ingredients of turmeric are curcumin, demethoxycurcumin, and bisdemethoxycurcumin (structures shown in Scheme 1).¹ The ratios of active components are highly variable based on plant growth conditions and processing.^{1,3} The purity of curcumin samples is tied to its common applications, which include pharmaceutical, food and beverage, and cosmetics industries.¹ Pharmaceutical grade curcumin has the highest purity and, as a result, is the most expensive.³ Nevertheless, the consumption of pharmaceutical grade curcumin accounts for the largest curcumin market share globally, with 54.08% market share in 2015.³ In North America, the market for curcumin accounted for the highest share in 2019, with a revenue percentage of 50.9%, and is forecasted to continue growing due to an

increased product demand as food and nutritional supplements and an organic additive in cosmetics.³ Synthetic curcumin can be obtained with the highest purity and a lower cost.^{3,4} However, despite the nearly miraculous biological properties,^{1,2} owing to its century-long use in Asia in the form of traditional herbal medicines and dietary supplements, curcumin is nonpatentable, which limits its appeal for further pharmaceutical development. In addition, curcumin demonstrates a variety of other limitations, with some noted examples being low water solubility, light sensitivity, low bioavailability in blood plasma, rapid clearance from the body, and its ability to act as a broad-spectrum inhibitor.^{1,2}

Due to a substantial cross-industry financial interest in curcumin, numerous reports have been published on the synthesis of derivatives.⁵ Synthetic modifications can be categorized as functionalization of aromatic rings (sidearm modification), modification of the central linker, or a combination of both (Scheme 1). The obtained curcuminoids have demonstrated an incredible potential in the pharmaceutical realm overcoming the pitfalls of curcumin itself.⁶ Despite the substantial developments in modifications of curcumin,⁷

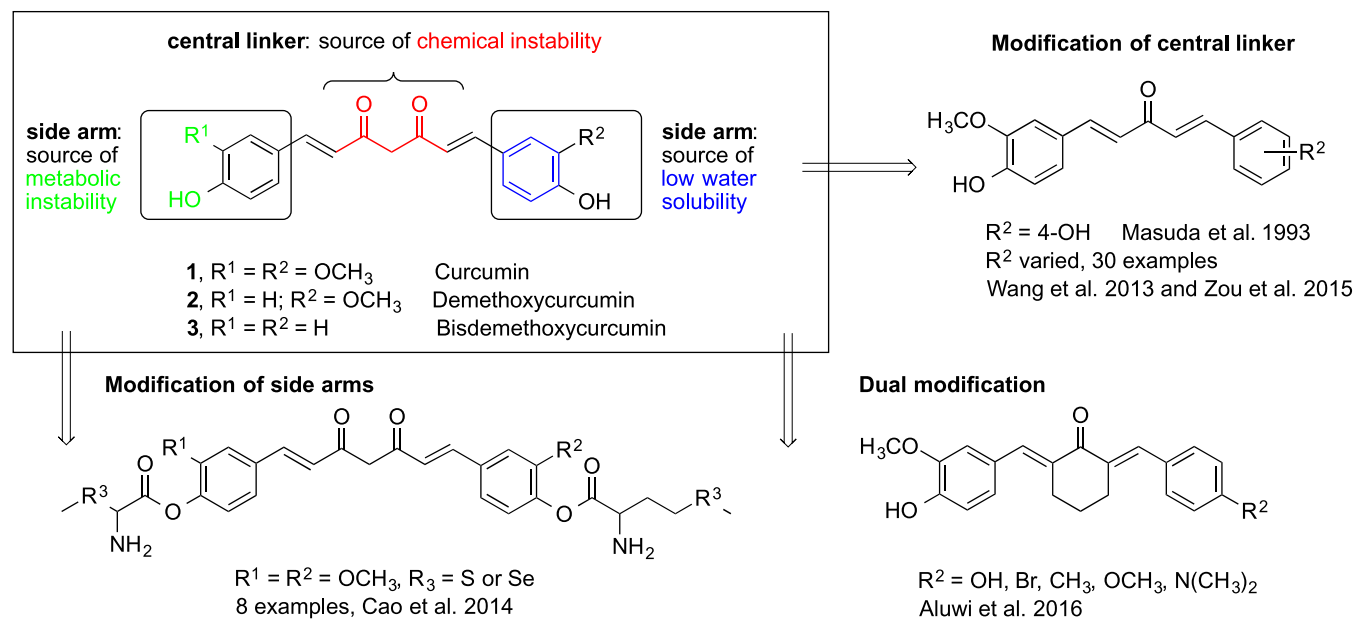
Received: December 15, 2021

Accepted: February 7, 2022

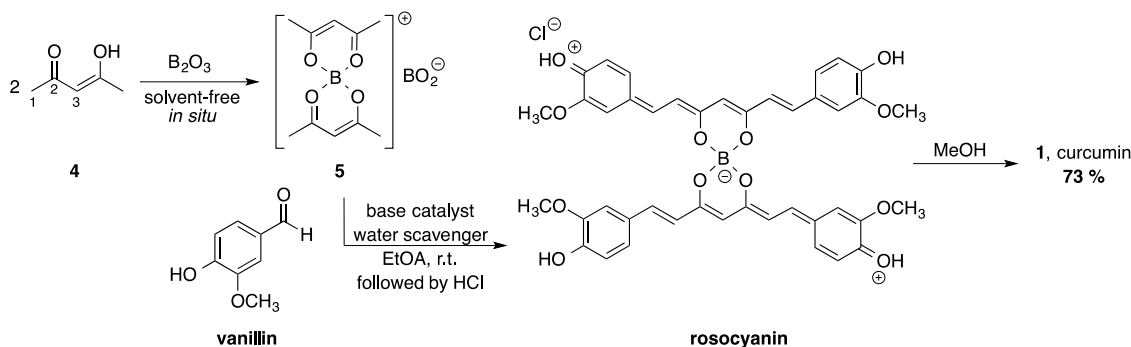
Published: February 21, 2022



Scheme 1. Chemical Structures of Active Components of Turmeric and Strategic Modifications toward Curcuminoids

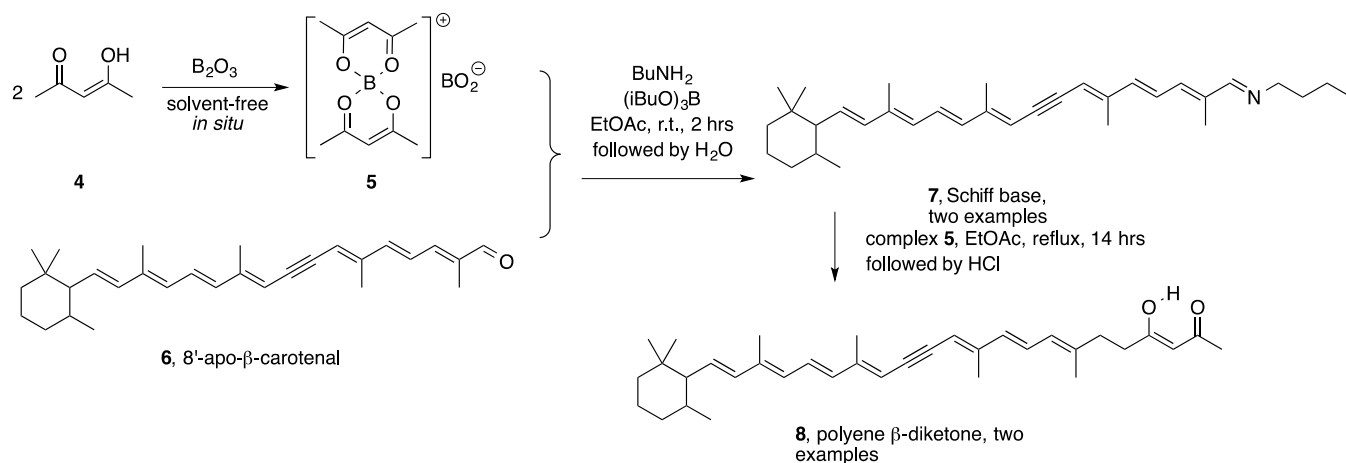


Scheme 2. General Procedure toward Curcumin and Its Close Analogues, Known as Pabon's Protocol

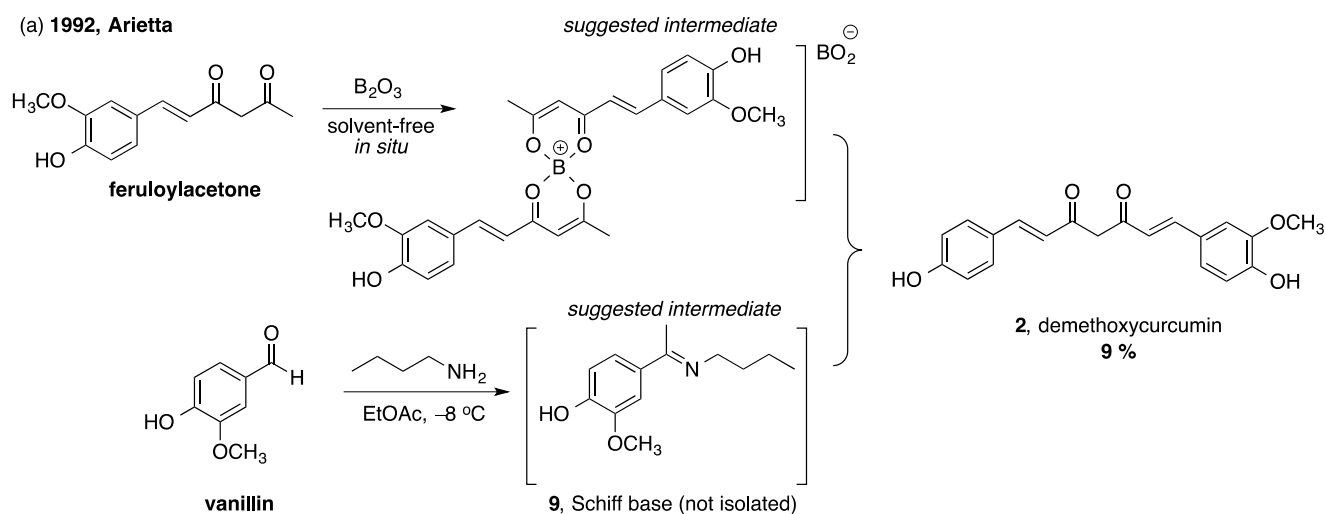


the synthetic procedures to these valuable compounds have not advanced and a vast array of curcuminoids are obtained by methods not that different from the approach reported by Pabon.⁸ As a consequence, synthetic efforts suffer from similar drawbacks as in the original report. Structural modifications of the aldehyde precursors are frequently accompanied by inexplicable substantial drops in yields.^{5b-d} Product isolation, with a few exceptions,^{5c} usually requires extensive multiple extractions, followed by recrystallization or column chromatography.^{5,6} The commercial availability of asymmetric curcuminoids is limited to a few examples, and at a relatively high price, limiting the availability of this resource to diverse research groups.¹ In a recent review,⁷ synthetic efforts of many research groups toward asymmetric derivatives of curcumin illustrating that the choice of a particular set of synthetic conditions on every step of the procedure, e.g., temperature, time, solvent, isolation, and purification, appear somewhat arbitrary and more representative of the culture of the particular group rather than the reaction in hand. Literature data contains limited information on the understanding of the reaction conditions, which is primarily based on the mechanism outlined by Pabon (Scheme 2).⁸ The formation of synthetic curcumin can be achieved by a one-step aldol condensation between vanillin (4-hydroxy-3-methoxybenzaldehyde) and acetylacetone (2,4-pentanedione), known as the

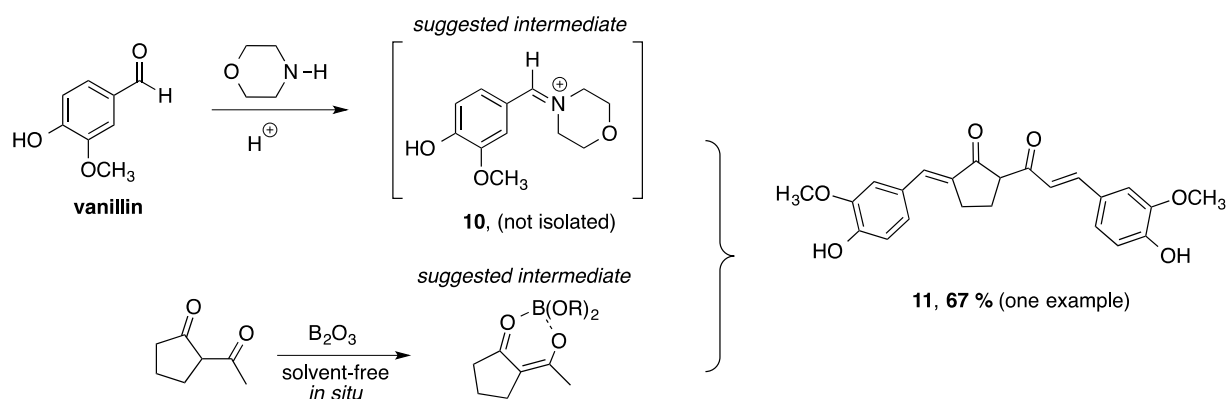
Claisen–Schmidt reaction. The method,⁹ originally developed by Lampe in 1910 and improved by Pavolini in 1937, produced curcumin in a 10% yield in one step but required an open flame for the success of the reaction. By introducing a borate ester, an amine, and conventional heating, Pabon achieved a 25–80% yield of curcumin under both solvent-free and solvent-based conditions.⁸ Moreover, the synthesis included several substituted benzaldehydes, thereby producing a small variety of curcumin derivatives and establishing the first general procedure toward this class of compounds.⁸ The protocol incorporates the conversion of enolic form 4 to intermediate 5 from acetylacetone and boric oxide in ethyl acetate followed by the addition of vanillin (Scheme 2).⁸ Formation of intermediate 5 prevents undesirable Knoevenagel condensation at the C-3 atom once exposed to base and aldehyde. The subsequent reaction is carried out in the presence of water scavengers, such as boric acid esters, as well as a base catalyst. Tri(isopropyl) borate and *n*-butyl amine produced the highest reported yield (80%) of curcumin.⁸ When the same protocol was applied to cinnamaldehyde, only the monocondensation product was isolated despite the lack of changes made to stoichiometric ratios of reactants. Similar attempts with furfural yielded product in a low yield (8%). Average reported yields ranged between 30 and 40% for other benzaldehyde derivatives.⁸ The solvent-based reactions con-

Scheme 3. Synthesis of Polyene β -Diketone and Isolation of Possible Active Intermediate—Schiff Base

Scheme 4. Suggested Mechanistic Steps or Intermediates in the Synthesis of Curcumin Analogues



(b) 2019, Mullins and Prusinowski



sistently outperformed solvent-free conditions. The need and type of supplementary reagents, such as amine catalysts and water scavengers, were investigated in relation to their impact on the product yield; however, their role in the stepwise mechanism is only suggested. The observation that primary or secondary amines are required for a successful synthesis is noted but is not further analyzed. No explanation is provided for inconsistent product formation (mono- versus diaddition), yield, or difficulty of product isolation.⁸

Several groups investigated solvent effects targeting the importance of product solubility in the formation of curcumin.^{8,10,11} The most relevant study¹⁰ includes a variety of solvents, polar and nonpolar, protic and aprotic, with dielectric constants ranging from 2.22 (1,4-dioxane) to 47.2 (DMSO), producing yields lower than the original 1964 Pabon protocol. The selection of a solvent is noted as essential for the reaction success from the beginning of the synthesis throughout the isolation and purification steps.¹⁰ The impact

of the solvent beyond the solubility and toward the efficiency of the base catalyst is mentioned without explanation.¹⁰ Reported complications including the increase of viscosity during the synthesis and formation of tarry, sticky, or gummy reaction mixtures are noted. The required use of large quantities of solvents either for the repeated recrystallization of filtrates or for column chromatography of concentrated solutions was described. The report¹¹ of high yields under continuous reflux on toluene or DMF is only marginally relevant toward the goals of this study due to the difference in their boron reagent.

The formation of acetylaceton–boron complex **5** was speculated⁸ based on the studies by Spicer with Strickland.¹² Although they have reported an extensive study of the chemical and physical properties of rosocyanin (Scheme 2), the structure of the proposed starting boron oxide–acetylaceton complex **5**, the key intermediate of the boron-bound monoaddition product, was not confirmed by crystallographic studies.¹² Later, John et al. proposed the base-catalyzed mechanism of the hydrolysis of rosocyanin to release curcumin along with Na[B(OH)₄].¹³ Considering that the majority of synthetic procedures toward curcumin or curcuminoids provide products upon treatment with hydrochloric acid, this mechanism would not seem applicable to these protocols. Chopra et al. speculated that the actual intermediate is a Schiff base formed by the substituted benzaldehyde and amine in the presence of a borate ester.¹⁴ Reaction of 8'-apo-β-carotenal **6** was carried out using tri(isobutyl) borate and *n*-butyl amine after the formation of complex **5** and did not result in the condensation of aldehyde (Scheme 3) but provided several Schiff base intermediates, e.g., compound **7**.¹⁴ Isolated compounds upon combining with the boric oxide complex of acetylaceton **5** in ethyl acetate under reflux for 14 h produced polyene diketones after treatment with HCl and crystallization from ethyl acetate (Scheme 3).¹⁴ Although speculated, similar imine compounds, e.g., **7**, were neither observed during the TLC monitoring of the reactions nor isolated for the synthesis of curcumin itself.

Later, the report of the low yielding synthesis of the asymmetric demethoxycurcumin **2** by condensation of the boron complex of feruloylacetone and *p*-hydroxybenzaldehyde (Scheme 4a) supported the speculation of the importance of the Schiff base formed by vanillin and *n*-butyl amine.¹⁵ The formation of an ionic iminium intermediate between vanillin and morpholine was also suggested in the synthesis of a curcumin analogue **10** (Scheme 4b) through an iminium ion-based mechanistic pathway.¹⁶

The solvent-free synthesis of curcuminoids was explored as part of ongoing efforts¹⁷ to expand the applicability of solvent-free approaches, toward small, biologically important molecules, as a means to develop greener, more atom-economical processes. Despite the report of the solid-state synthesis of curcumin and related compounds,¹⁸ to the best of our knowledge, there has been no investigation of the applicability of solvent-free approaches for the syntheses of such compounds. The present combined mechanistic and crystallographic study has yielded crystal structures of three curcuminoids and one reaction intermediate. These synthetic efforts were paired with the computational modeling of the relevant compounds. Previous computational studies of curcuminoids have been primarily focused on two veins: (1) prediction of the biological properties via docking studies¹⁹ and (2) prediction of their photophysical properties via

TDDFT methods.^{20,21} Additionally, computational methods were used to assess the validity of the catalytic role of the amine, as well as to ascertain the plausibility of an iminium ion intermediate in the proposed catalytic cycle. To the best of our knowledge, there has been no hybrid experimental–computational investigation of the relationship between isolated yields, structural features, and reaction conditions in the solvent-free synthesis of curcumin and its analogues.

SYNTHETIC RESULTS AND DISCUSSION

Development of Curcumin Solvent-Free Synthesis.

Initial studies looked at the reaction of vanillin, acetylaceton, boron trioxide, tri(*n*-butyl) borate, and catalytic *n*-butyl amine under solvent-free conditions (Table 1). Optimal yields were

Table 1. Optimization of Solvent-Free Synthesis of Curcumin 1

entry	(<i>n</i> -BuO) ₃ B ^a	T (°C)	time (h)	yield (%)
1	1.0	55	18	11.7
2	2.1	55	18	44.7
3	3.0	55	18	68.6
4	4.0	55	6	40.2
5	4.0	55	18	82.2
6	4.0	55	36	67.4
7	1.0	75	18	33.9
8	2.1	75	18	40.7
9	3.0	75	18	63.6
10	4.0	75	6	49.3
11	4.0	75	18	77.8
12	4.0	75	36	73.8
entry	B ₂ O ₃ ^a	T (°C)	time (h)	yield (%)
13	0.2	55	18	23.3
14	0.4	55	18	67.0
15	0.7	55	18	82.2
entry	vanillin ^a	T (°C)	time (h)	yield (%)
16	2	55	18	82.2
17	3	55	18	79.3
18	4	55	18	63.3

^aEquiv is calculated per quantity of acetylaceton used.

obtained using 4.0 equiv of borate and 0.7 equiv of B₂O₃ (entries 5 and 11). Alteration of a boron source to boric acid was not investigated under solvent-free conditions as this modification under the solvent-based method resulted in a low product yield, e.g., 5% for curcumin **1**, and required extensive column chromatography during isolation.²² Modification of a boron source to boron trifluoride reported by others^{23–25} was not investigated under solvent-free conditions due to the lack of obvious synthetic advantages. High 80–90% yields of final products **1–3** (Scheme 1) required moisture-sensitive reagents, anhydrous synthetic conditions, and substantial chromatographic separation.²³ Modification of the solvent provided BF₂ complexes of curcuminoids **1–3** as insoluble solids.²⁴ The hydrolysis of the corresponding BF₂ complexes to provide the final curcuminoids is limited and not always reproducible even under solvent-based conditions.²⁵

An optimization of reaction parameters was conducted, and the results are summarized in Figure 1 and Table 1. Stepwise modification of borate ester quantities was coordinated with an alteration of time and temperature until optimal conditions were found. Modification of the reagent ratio was achieved by

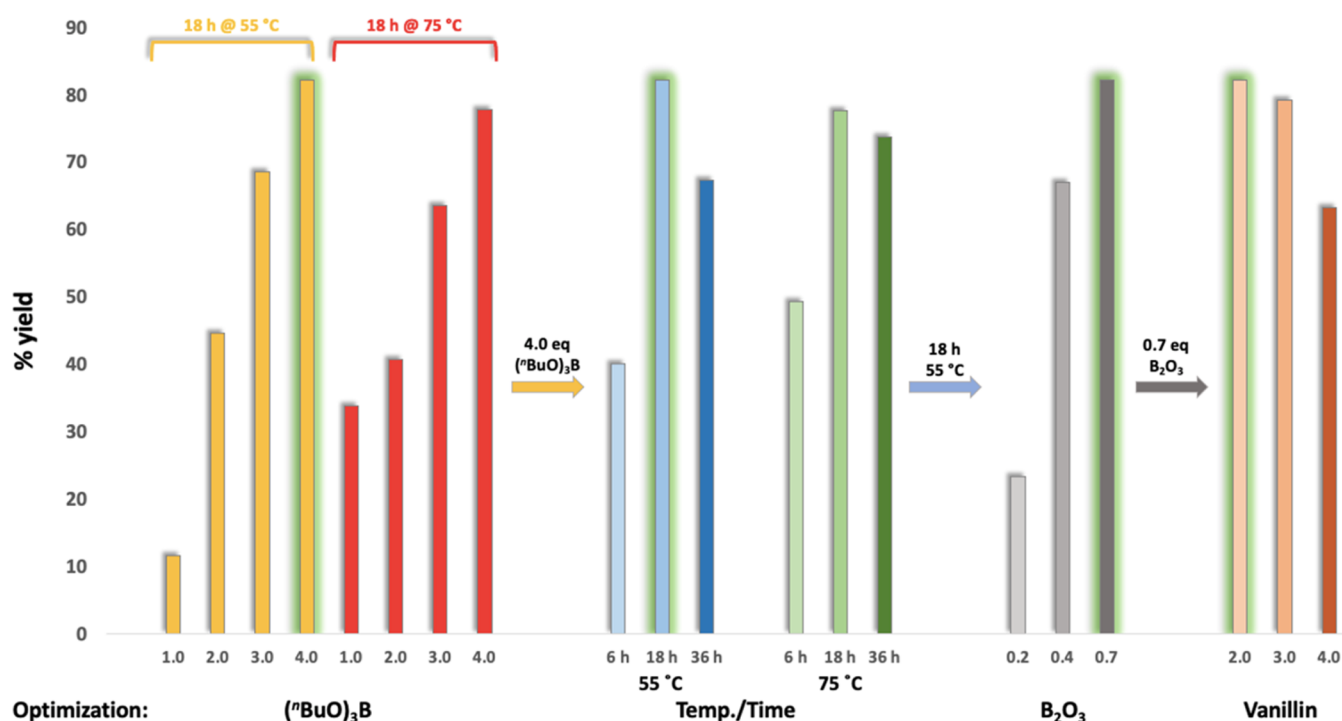


Figure 1. Optimization of the solvent-free methodology using acetylacetone **4** (2.5 mmol), butyl amine catalyst (10 mol %), varied amounts of vanillin, B₂O₃, and tri(*n*-butyl)borate under varied temperatures and times.

the alteration of quantities of vanillin. Catalytic amounts of boron oxide were varied since it is commonly used in stoichiometric quantities. The nature of the amine was not modified as it was previously extensively investigated under solvent-based conditions (Pabon⁸ 1964 and Krakov¹⁰ 1997). The impact of the amine catalyst amounts demonstrated little to no effect on product yield.²⁶ Therefore, *n*-butyl amine in catalytic (10 mol %) quantities was used for all reactions.

Tri(*n*-butyl)borate was used for all experiments, with the exception of tri(isopropyl)borate ester implemented in the mechanistic investigations to allow the tracing of *n*-butyl amine during *in situ* experiments. Several studies of borate ester substituent effects demonstrate a small impact on product yields,^{5b,8,10} and the majority of syntheses employ tri(*n*-butyl)borate ester.^{5,7}

Due to solvent-free conditions, monitoring of reaction mixtures could be performed using TLC or ¹H NMR spectroscopy at any point in the synthesis. After product formation was confirmed, reaction mixtures were quenched with water. Contrary to traditional approaches, no extensive extractions were required in this solvent-free method. The product was isolated using vacuum filtration resulting in curcumin **1** (Scheme 1) in high purity without the need for further recrystallization or column chromatography.

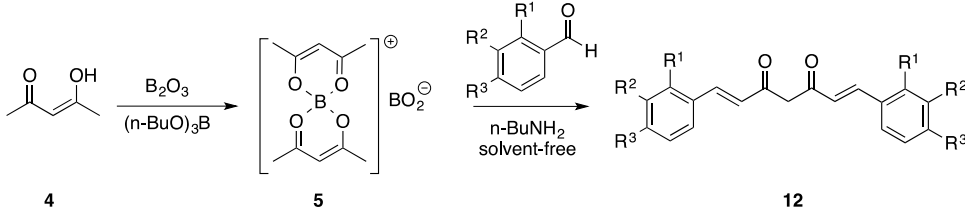
Variation of molar equiv of (*n*-BuO)₃B ranging from 1.0 to 4.0 (reaction temperature of 55 °C and time of 18 h were maintained throughout all trials) produced curcumin with yields varying from ~11 to 82% (Table 1, entries 1–6). In all reactions, a mixture of acetylacetone **4**, B₂O₃, and (*n*-BuO)₃B initially was heated in a vial at 55 °C for 20 min, producing a nearly homogeneous suspension of intermediate **5**. The increase of temperature to 75 °C generally resulted in a relatively small decrease in the overall yield (Table 1, entries 7–12), providing curcumin in a 34–78% yield. The optimal conditions observed at 75 °C employed 3 or 4 equiv of borate

ester. An exception to this trend was observed when 1.0 equiv was used; however, this could be explained by the decreased viscosity at 75 °C that facilitates reaction mixing. Dry addition of vanillin and *n*-BuNH₂ catalyst was used in all reactions to ensure a consistent volume of mixtures. The range of yields narrowed at higher temperatures and was less dependent on the equiv of borate ester applied. Variation of time at each temperature provided lower product yields when either shorter or longer times were used (Table 1, entries 4–6 and 10–12). On average, shorter times were more detrimental to isolated yields than were longer reaction times (Table 1, entries 4 and 6, 10, and 12). Aligning with the goal of the optimized protocol instead of optimizing individual yields, 18 and 36 h were consistently applied for the next steps.

Using optimized reaction conditions (Table 1, entry 5), the effect of varying quantities of boric anhydride and vanillin was studied. Both components are solids and under solvent-free conditions can severely impact the stirring of the reaction mixture. Reduction in the amount of B₂O₃ applied corresponded to a drastic drop in product yield (Table 1, entries 13 and 15). Product isolation was performed as described above. The formation of a Knoevenagel condensation product was not observed even when decreased amounts were used, and unreacted aldehyde was isolated upon hydrolysis with water and ethyl acetate mixture.

Considering the catalytic use of boron oxide and butyl amine, one can expect that increasing aldehyde quantities may increase the curcumin yield. Krakov comments that the depletion of aldehyde through side reactions can occur.¹⁰ The impact of vanillin ratios was studied after the formation of intermediate **5** was observed; however, the quantities of *n*-BuNH₂ were not modified. The increase of vanillin equiv from a stoichiometric ratio to 3 equiv demonstrated no significant change in the isolated yield of curcumin **1** when 3 equiv was used (Table 1, entry 17). Product yield decreased somewhat

Table 2. Expansion of the Solvent-Free Protocol for the Preparation of Curcuminoids



Entry	Code	Substituents			Isolated yields (%)			
		R ¹	R ²	R ³	55 °C, 18 h	55 °C, 36 h	75 °C, 18 h	75 °C, 36 h
1	12a	H	H	H	21.2	14.1	14.3	11.0
2	12b	NO ₂	H	H	30.6	27.2	34.5	44.5
3	12c	H	NO ₂	H	38.2	41.8	39.5	48.7
4	12d	H	H	NO ₂	28.4	17.2	30.1	39.7
5	12e	Cl	H	H	40.8	30.8	46.3	39.4
6	12f	H	Cl	H	57.5	70.7	81.0	70.7
7	12g	H	H	Cl	67.5	80.0	69.7	60.9
8	12h	OCH ₃	H	H	52.2	58.2	47.3	68.2
9	12i	H	OCH ₃	H	51.2	54.3	41.3	56.1
10	12j	H	H	OCH ₃	62.7	69.3	64.6	74.1

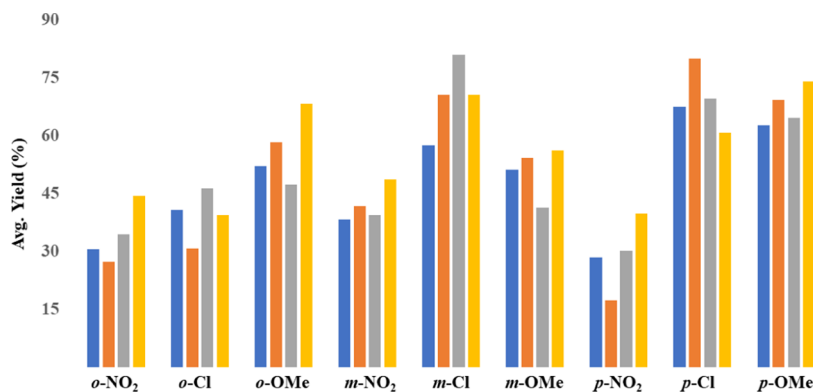


Figure 2. Versatility of the solvent-free methodology—systematic comparison of product yields.

moderately when 4 equiv was applied (Table 1, entry 18). However, this observation could at least, in part, be attributed to the additional required recrystallization of the product to remove the excess of unreacted aldehyde present in the product after vacuum filtration based on the TLC data.

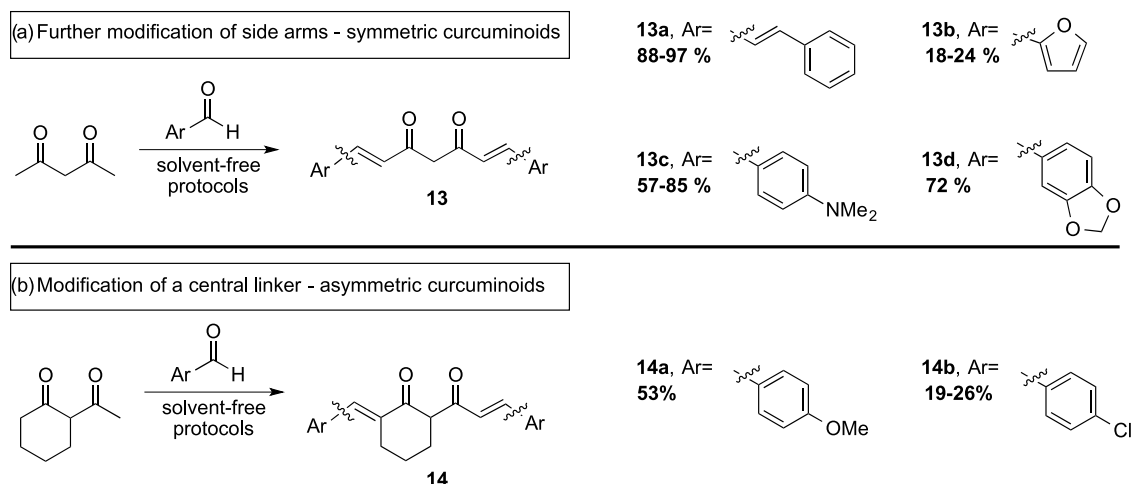
In summary, the developed solvent-free methodology has provided curcumin **1** with yields far exceeding the one reported by Pabon (43%)⁸ with a substantial decrease in effort required for the isolation and purification of the product. In some cases, the obtained product yields were better than those observed for solvent-based methods.^{8,10,11}

Study of Versatility of Solvent-Free Method to Obtain Symmetric Curcuminoids. To study the applicability of the solvent-free method to obtain products other than curcumin itself, the effect of a functional group in substituted benzaldehydes was systematically investigated. Using optimized conditions and varying the type and attachment of the functional group, a variety of curcuminoids **12a–j** were obtained (Table 2 and Figure 2). The versatility of the solvent-free approach was investigated and the performance of the starting substituted benzaldehyde was systematically compared under mild and high heating conditions. Based on a combination of literature data and our observations, well-performing starting materials were selected—the anisaldehyde

series, poor-performing ones—nitrobenzaldehydes, along with those that have demonstrated a mixed performance under different methods—chlorobenzaldehydes. Benzaldehyde itself was included as a benchmark for the functional group impact.

Substitution of vanillin with anisaldehydes did not require the alteration of addition procedures despite the change in the physical state between these two starting materials. Initial trials were conducted at 55 °C for 18 h using anisaldehydes, with all other parameters identical to the previously described curcumin synthesis itself. Although a slight dilution occurs due to the volume increase, it did not have a significant impact on the appearance or performance of the reactions. Initially, the progress of reactions was monitored using TLC hourly for the first 6 h, and although the formation of the product was detected, an incomplete conversion of starting aldehydes was observed. An extension of the time to include overnight stirring demonstrated an increased conversion on the TLC scale. The analysis of ¹H NMR of the crude mixture independently confirmed the decrease of an aldehyde, $-C(O)H$, signal at ~ 9 ppm while exhibiting the strong trans-coupling signals of the product along with other signals. Relative quantitative analysis of the exact ratios on the NMR scale was not possible due to an overlap of trans-coupling and aromatic signals. Attempts to increase isolated yields separately using both increased reaction

Scheme 5. Expansion of Solvent-Free to Include Further Sidearm and Central Linker Modifications



times (55 °C and 36 h; Table 2, column 8) and increased temperatures (75 °C and 18 h) (Table 2, column 7) were made. The impact of those changes was not always positive (Table 2, entries 1 and 5). Use of unsubstituted benzaldehyde resulted in the decreased yield of 12a when time and temperature increases were applied. However, on the introduction of the *ortho*-nitro group in the starting aldehyde for 12b, the temperature increase had little to no effect, but the extended reaction time resulted in a nearly doubled overall yield. Trends for 12f and 12g were reversed, with the formation of 12f being promoted by the increased temperature, while 12g was produced in a higher yield after prolonged reaction times. Although the reproducibility of each experiment was on an acceptable level, the overall pattern of yields seemed to be highly dependent on the functional group present in aldehyde as well as its location. To identify trends in the performance of aldehydes, data were grouped together to illustrate the effect of the functional group type and its location (Figure 2). Although in some cases (e.g., *p*-nitrobenzaldehyde, 17.2%; Table 2, entry 4; Figure 2) an isolated product yield was lower than desired, this was easily overcome by a modification of a single reaction parameter.

No strong correlation between the use of a particular set of reaction conditions (e.g., mild heat versus high heat) on the reaction yield was identified. When using nitro- or methoxy-substituted benzaldehydes, the best performance was observed for longer reactions at higher heat (Table 2, entries 2–4 and 8–10; Figure 2). However, for chloro-substituted benzaldehydes, the best product yields were obtained when using higher heat at a shorter reaction time, with the exception of *p*-chlorobenzaldehyde (Table 2, entries 5–7; Figure 2). It is worth mentioning that the use of temperatures higher than 75 °C was found to be unsuccessful resulting either in decomposition or in intractably thickened reaction mixtures. The increased viscosity complicated the workup and required labor-intensive separation of components without substantial impact on the desired product yields. The maximum duration of 36 h was chosen for practical reasons, although it could be considered as a parameter worth modifying if a particular reaction results in a lower yield in the future. In general, the direct comparison of the functional group for the solvent-free protocol was on par with that reported previously for the solvent-based reactions, with anisaldehydes generally outperforming the nitro- and chloro-substituted aldehydes to

produce yields of a wider spectrum. No single trend connecting the variation of the substituent location and product yield (Figure 2) was identified. Although *para*-substitution promoted the product formation when a methoxy- or a chloro-group was tested, the corresponding nitro-compound was below those observed for the *ortho*- and *meta*-substituted analogues (Figure 2). This in-depth comparison of yield outcomes per functional group location was also complicated by the varied performance of selected aldehydes, with the modification of reaction parameters such as temperature and time. Overall, the data support the general trend observed for the solvent-based synthesis of curcuminoids that the prediction of the anticipated performance of an aldehyde based on its structural build or electronic property is relatively complicated. The data also demonstrate the efficiency of solvent-free methodology, in particular, mild heat (55 °C) and longer time (36 h), toward the formation of a curcuminoid with a moderate to good yield regardless of the substitution type or its location.

Expansion of Solvent-Free Methodology. The observed performance of the protocol encouraged us to expand the synthetic scope to include substituted benzaldehydes with different functional groups (Scheme 5a) and a modification of a central linker (Scheme 5b). Based on previous results, a longer reaction time of 36 h was employed while testing both temperatures (55 and 75 °C). The selected set of parameters was best suited for the direct assessment of the method applicability as well as the ease of translation to new substrates (Table 3). For further modification of sidearms, cinnamaldehyde, furfural, *p*-dimethylaminobenzaldehyde, and piperonal were included. The protocol provided corresponding com-

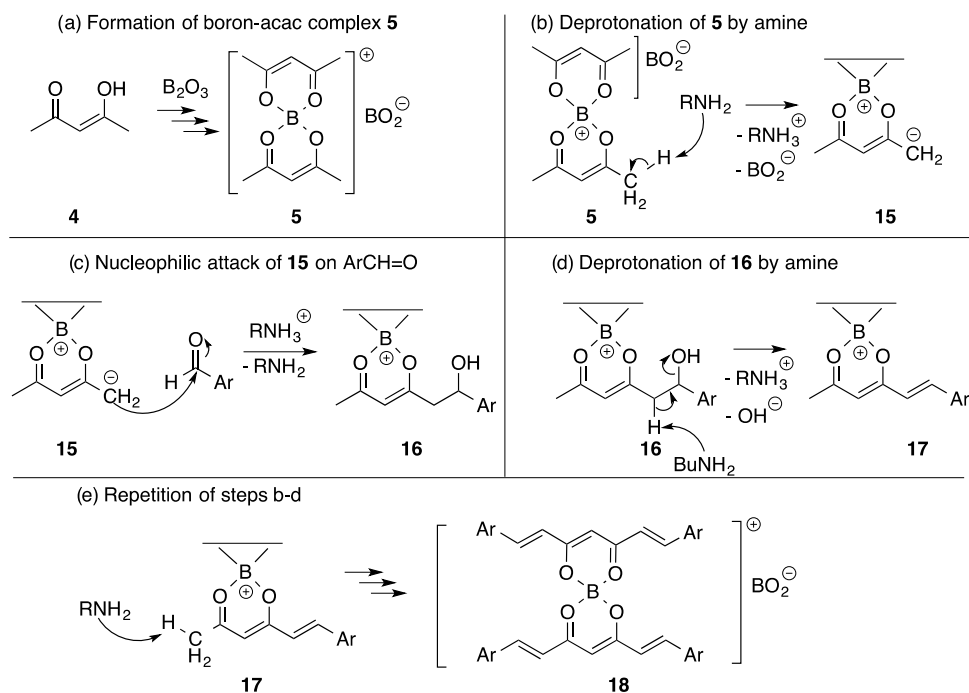
Table 3. Reaction Outcomes for the Expansion of Solvent-Free Methodology

entry	compound	time = 36 h isolated yield (%)	
		55 °C	75 °C
1	13a	97.6	88.3
2	13b	24.3	18.2
3	13c	57.9	84.5
4	13d	73.4	72.7
5	14a	53.8	52.8
6	14b	26.3	19.2

Table 4. Noted Limitations of the Solvent-Free Approach

entry	code	substituents			isolated yields (%)			
		R ¹	R ²	R ³	55 °C, 18 h	75 °C, 18 h	55 °C, 36 h	75 °C, 36 h
1	12k	OH	H	H	traces	traces	traces	traces
2	12l	H	OH	H	26.11	25.17	32.41	23.64
3	12m	H	H	OH	31.40	16.32	28.71	19.22

Scheme 6. Summary of Anticipated Mechanistic Benchmarks Based on the Proposed Intermediates 5 and 18



pounds **13a**, **13c**, and **13d** in good to excellent yields (Scheme 5a; Table 3, entries 1, 3, and 4) and compound **13b** in a low ~20% yield; however, it still exceeds the 8% reported by Pabon⁸ and did not require substantial alteration of a workup procedure on our part.

An increase in the conjugated system, as in the case of cinnamaldehyde, had a dramatic effect on the isolation of product **13a** (Scheme 5a; Table 3, entry 1). Both reaction conditions provide an excellent yield; for comparison, Pabon⁸ reported an isolated yield of 29% for the same compound when conducting the reaction at 50 °C in ethyl acetate for 4 h. Although, in part, the isolated yield could be explained by the extension of the reaction time, the similar excellent performance of the method in the case of piperonal indicates the benefits of solvent-free conditions (Table 3, entry 4). The isolated yield of product **13d** was ~73% for both temperatures compared to the previously reported⁸ 59%. It is interesting to note that the isolated yield for reactions of *p*-*N,N*-dimethylbenzaldehyde varied significantly, with a lower temperature resulting in a substantial decrease in the product yield (Table 3, entry 3). However, in both protocols, product **13c** was isolated with a better yield than previously reported (36%).⁸

Translation of the solvent-free protocol to obtain asymmetric compounds was achieved by substituting acetylacetone with 2-acetylcylohexanone (Scheme 5b). Two aldehydes, previously performed best under experimental conditions (see Figure 2), were tested, while ratios of boric anhydride, borate ester, and *n*-butyl amine catalyst were used as described above

for the curcumin synthesis itself. Stoichiometric ratios of a diketone linker and a corresponding aldehyde to ensure the possibility of a complete conversion and simplify reaction monitoring were applied. The data (Table 3, entries 5 and 6) demonstrate the general ease of translation of the current protocol to obtain asymmetric curcuminoids **14a,b**. It appears that on average, lower yields were obtained even for prolonged reaction times or elevated temperatures. Interestingly, *p*-chlorobenzaldehyde did not perform as well as expected based on the data collected for acetylacetone reactions (Table 3, entry 7) where symmetric product **12g** was isolated in ~70–80% yields across several solvent-free protocols, while the analogous asymmetric **14b** was produced in less than half the yield (~20–30%; Table 3, entry 6). Considering all reactions were conducted without a solvent, further investigation to overcome the low yield limitation, e.g., the impact of borate ester, might be required to enhance yields due to the potentially lower solubility of starting compounds.

Method Limitations: Hydroxy-Substituted Starting Materials. The general success of the solvent-free approach did not translate to reactions involving hydroxy-substituted benzaldehydes as starting materials (Table 4; for synthesis, see Scheme 4). In particular, all four protocols failed to provide appreciable amounts of the isolated product for the *ortho*-hydroxybenzaldehyde starting material (Table 4, entry 1). “Traces” indicate that a majority of the starting material, in either the free or B-bound form, was isolated upon quenching of reaction mixtures using vacuum filtration by the addition of water–ethyl acetate mixture. Although alterations of the

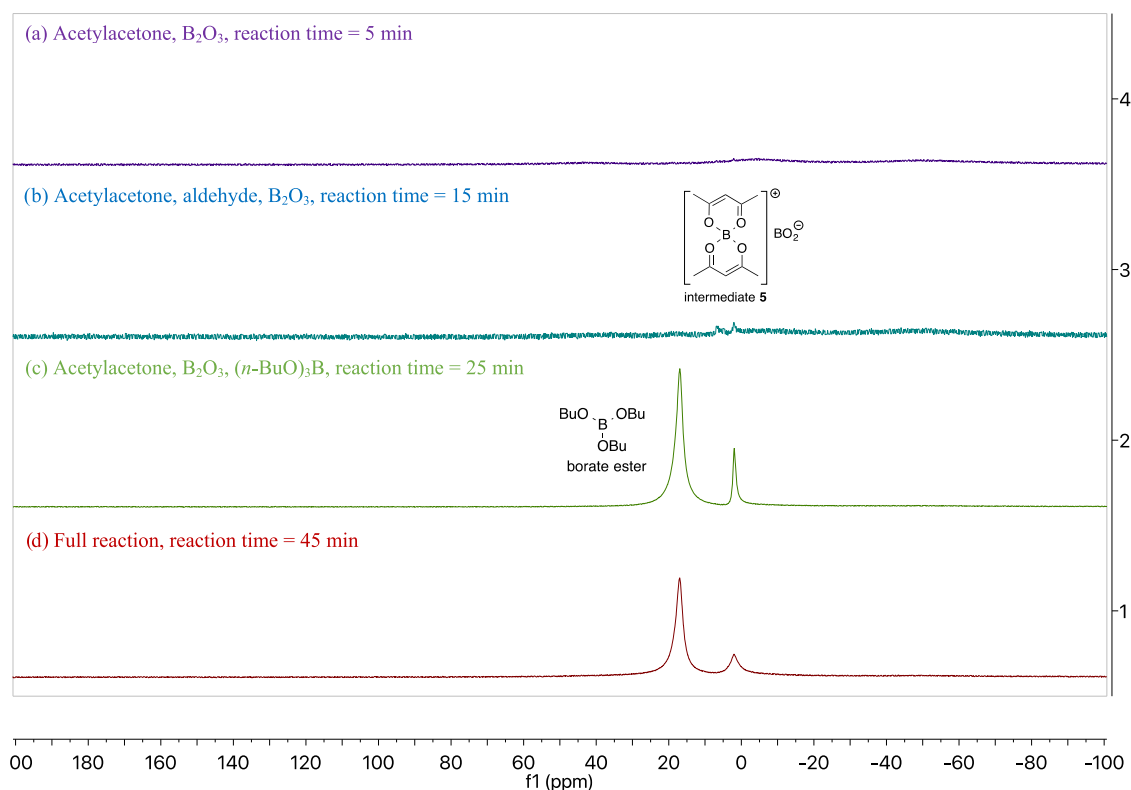


Figure 3. $^{113}\text{B}\{^1\text{H}\}$ NMR data supporting the *in situ* formation of intermediate 5.

isolation procedure (see the [Experimental Section](#)) allowed us to isolate the desired compound, this limited the method. *Meta*- and *para*-hydroxybenzaldehydes provided products without alteration of the workup protocol, but yields remained low ([Table 4](#), entries 2 and 3). These observations led us to question the general understanding of the mechanism of the reaction and led to the mechanistic investigations described herein.

Mechanistic Study and Isolated Intermediate. The current understanding of the mechanism for the formation of curcumin and related compounds is in large part based on the ideas proposed by Pabon.⁸ To the best of our knowledge, there is no published step-by-step synthetic mechanistic investigation for the formation of curcumin or related compounds using vanillin, boric anhydride, borate ester, and amine catalyst under solvent-based or solvent-free conditions.

Using a basic understanding of the condensation reactions and assuming a strict assignment of the amine solely as a base, one can identify the main benchmarks of the potential mechanism ([Scheme 6](#)) as follows: (a) formation of the boron–acetylacetone complex **5**, (b) deprotonation of intermediate **5** by amine producing enolate-type intermediate **15**, (c) nucleophilic attack on aldehyde resulting in the monocondensation product **16**, (d) repeat of the deprotonation step providing intermediate **17**, and (e) repeat of steps **b–d** resulting in rosocyanin-type compound **18**. Cleavage of **18** under acidic or basic conditions would release free curcuminoid; this step is not shown as it is not applicable to the solvent-free protocol. The outlined step-by-step formation of the curcuminoid skeleton in large part is based on the structures of intermediates **5** and **18** and, to the best of our knowledge, has not been discussed before. The formation of an intermediate **5** eliminates the potential for Knoevenagel

condensation due to preceding deprotonation at the methylene carbon. Pabon⁸ used the specific language “the compound probably has the structure” and clearly stated that he was only speculating on the formation of intermediate **5**; however, it was later reinforced by others.^{14–16} Although the formation of complex **5** is widely accepted,⁷ to the best of our knowledge, it has not been isolated and there is no reported crystal structure of this compound. In addition, the common language used by others when discussing the role of boric anhydride usually refers to it as a catalyst despite its use in stoichiometric quantities. Intermediate **18** is a reasonable mechanistic outcome of the reaction progress and resembles the structure of rosocyanin. However, the role of this amine in the process is unclear. Amine is usually listed as a catalyst or a base source; however, experimental data of Krakov¹⁰ and Pabon⁸ independently demonstrated that only primary and secondary amines are successful catalysts in the reaction. In addition, the emphasis on maintaining a low and consistent concentration of amine was noted but the recycling of the catalyst has not been previously discussed.

The stepwise mechanism is clearly limited to the understanding of the actual role of the interchange of compounds involved. Therefore, potential catalytic cycles in the curcuminoid synthesis were identified. Taking advantage of the solvent-free method, the exchange of the functional groups using reaction samples was monitored by NMR. The initial attempts focused on the confirmation of the formation of complex **5**. After mixing acetylacetone and boric anhydride, the paste was analyzed using ^{11}B NMR spectroscopy ([Figure 3](#)). Although the formation of complex **5** was speculated⁹ and is widely accepted, to the best of our knowledge, it has never been isolated. Reaction mixtures leading to products curcumin **1** and curcuminoids **12h–j** were used as model experiments. A

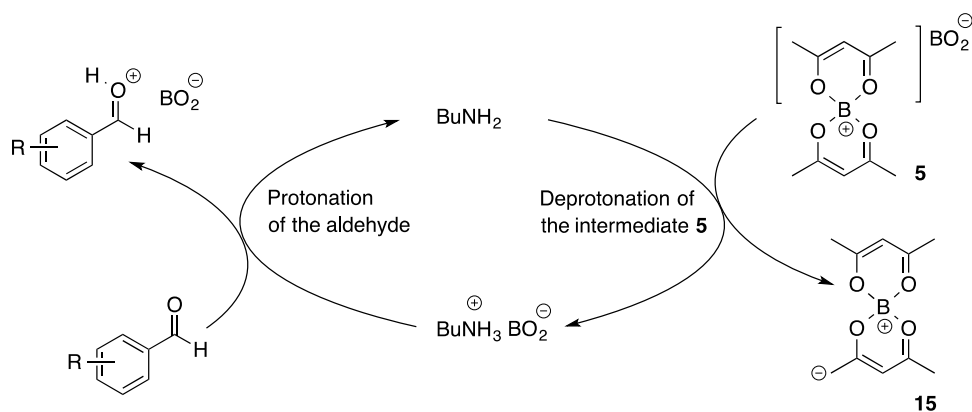


Figure 4. Use and regeneration of an amine catalyst in a general curcuminoid synthesis.

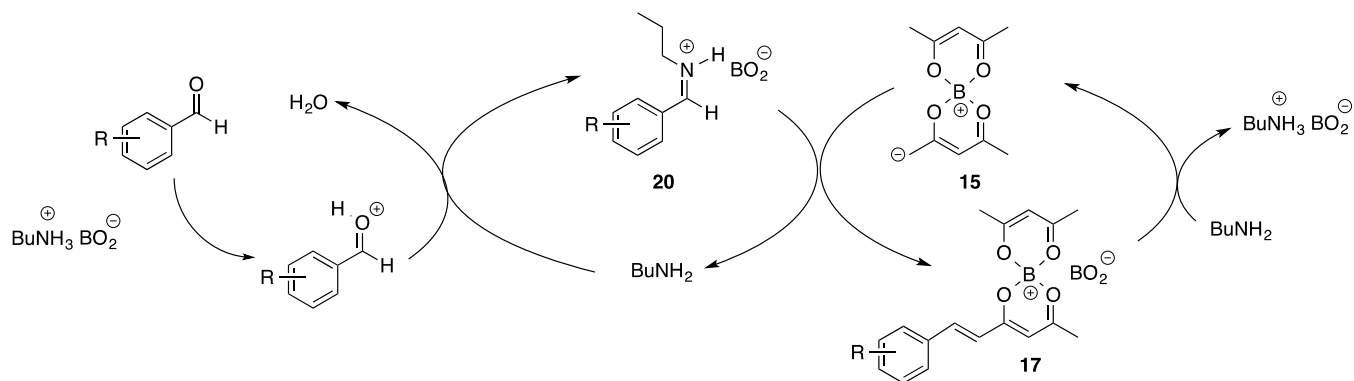


Figure 5. Proposed alternative role of the amine as a catalyst in the synthesis of curcuminoids.

mixture of acetylacetone **4** and B_2O_3 in stoichiometric amounts was combined at room temperature and stirred for 10 min. The reaction produced a homogeneous paste; after heat release ceased, a sample was dissolved in $CDCl_3$ and analyzed by NMR (Figure 3a,b). Poor solubility of complex resulted in a high signal-to-noise ratio, but the data demonstrate a change in the boron environment and the presence of two inequivalent boron atoms. After the addition of $(n-BuO)_3B$ occurred, the solubility of intermediate **5** had drastically increased, allowing for the improvement of spectrum quality (Figure 3c). The sample was taken as an aliquot via syringe and transferred into an NMR tube followed by the addition of $CDCl_3$ through a septum. The reaction sample was heated at $55\text{ }^\circ\text{C}$ for approximately 20 min, producing a somewhat homogeneous solution of intermediate **5** in borate ester. The signal of complex **5** modified upon the addition of borate ester, however, remained relatively unchanged as time progressed (Figure 3d). Attempts to isolate intermediate **5** by the interruption of reaction mixtures resulted in the isolation of boric acid, H_3BO_3 , as a previously unreported polymorph.

Once the formation of intermediate **5** is achieved, the aldehyde is introduced along with the water scavenger and amine. Keeping in mind that the amine is listed as a catalyst and a base and used in catalytic amounts, there should be a regeneration pathway for the amine to undergo a reversible acid–base interaction. Keeping those factors in hand, a catalytic cycle involving an aldehyde, intermediate **5**, and an amine (Figure 4) was proposed. For simplicity, a generic aldehyde and *n*-butyl amine were used. However, the same catalytic cycle could be easily translated to the use of another amine. Taking a deeper look at the proposed steps, it is not

obvious why primary and secondary amines seem to outperform tertiary amines in the reaction, a significant experimental observation previously noted by others.^{8,10}

Literature data^{8,14–16} suggest the possibility that prior to the reaction of an amine with intermediate **5**, it undergoes Schiff base formation with the aryl aldehyde, $ArCH=O$. Several experimental observations support this idea. For example, a drastic color change to blood red occurs nearly instantly upon the addition of the first equivalent of a base catalyst to the reaction mixture. Although one can argue that the transition of curcuminoids to basic pH could be attributed to the observed color change, at that time, no curcuminoid is present in the mixture according to TLC and NMR analysis. The same color change pattern is also observed when imine is synthesized independently. The possibility of converting imines to the corresponding curcuminoids upon reaction with complex **5** was independently confirmed by Chopra¹⁴ for solvent-based conditions and by us for solvent-free conditions. Since the imine (or iminium ion) formation can only occur with primary (or secondary) amines, in retrospect, it is not surprising that tertiary amines have been reported to be ineffective catalysts for curcuminoid formation. To the best of our knowledge, although the imine formation was speculated^{14–16} to include the iminium ion as an intermediate for the synthesis of an asymmetric curcuminoid with the aid of morpholine, there have been no investigations of the *in situ* formation of imine/iminium-type intermediates in curcumin reaction mixtures. There have been no attempts to propose an iminium-based catalytic cycle to explain the role of the amine and supporting compounds. Keeping in mind the protonation/deprotonation role of amine (outlined in Figure 4) and adding the adjoining

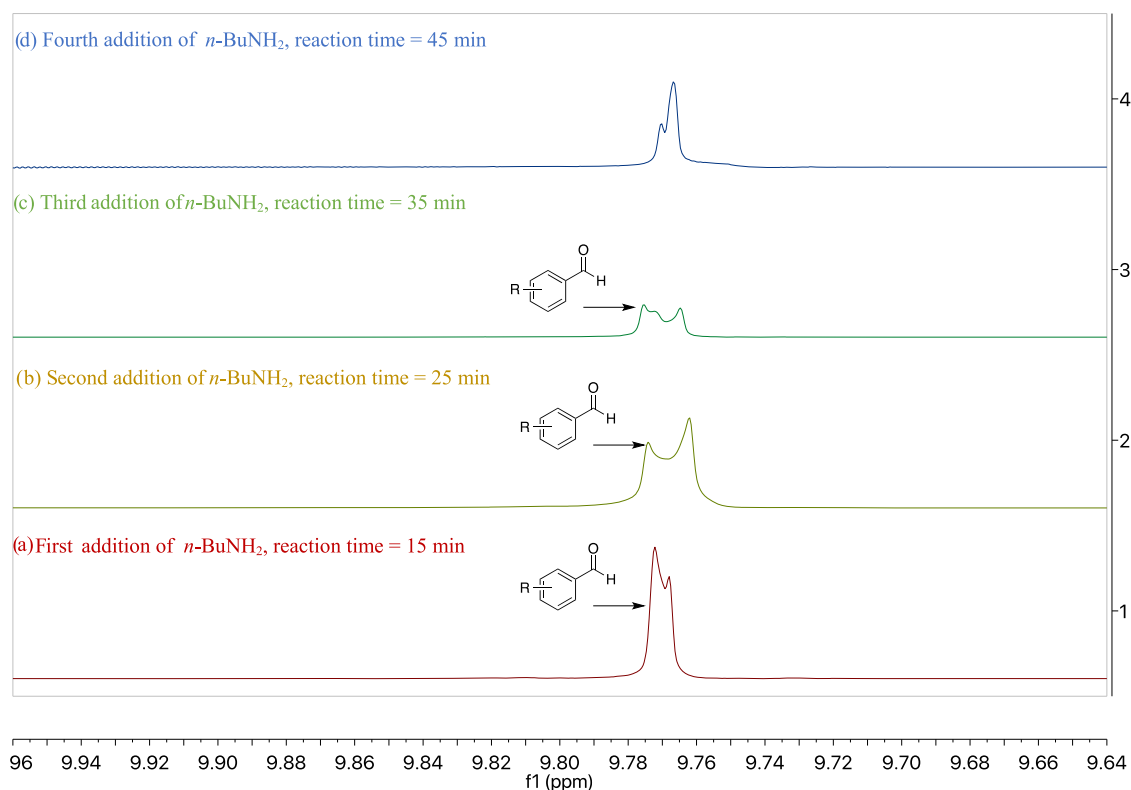


Figure 6. ^1H NMR monitoring of the *in situ* progress of curcumin **1** formation.

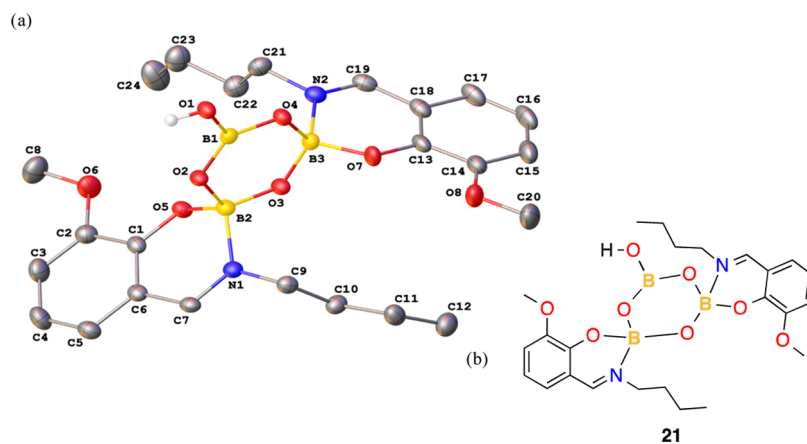


Figure 7. (a) Molecular drawing of **21**·0.94 CH_2Cl_2 with the solvent molecule of dichloromethane omitted. All non-H atoms are shown at 50% probabilities (all H atoms bound to C atoms are omitted) and (b) molecular diagram of **21**.

cycle to account for the interaction of aldehyde and amine, it is possible that the exchange of species follows the three-component catalytic cycle (Figure 5). The new cycle fits in between the protonation of aldehyde (shown on the left) and the formation of the monoaddition product **15**. It is also in line with the experimental observation that color change prior to the attachment of an aldehyde to the acetylacetonate moiety can occur. The deprotonation of complex **5** is not included in the depicted cycle but is illustrated previously (Figure 4).

Due to the solvent-free conditions, the transformation of reactants using ^{11}B and ^1H NMR was monitored. To avoid the complication of stirring in an NMR tube, mechanistic studies were conducted using a full-scale reaction mixture setup. As a result, the reaction mixture consisting of acetylacetone **4**, B_2O_3 , and $(n\text{-BuO})_3\text{B}$ was combined at room temperature and stirred

for 10 min to achieve a nearly homogeneous solution. A sample was taken to confirm a change of the boron environment prior to proceeding to the next step. After the formation of complex **5** was confirmed by NMR, full amounts of vanillin or *ortho*-vanillin were added dry, followed by the first addition of $n\text{-BuNH}_2$ using a syringe through a septum (Figure 6a). The full amount of amine (10 mol %) was divided into four portions (2.5 mol % each) to allow the stepwise monitoring of changes; the alternative, extended dropwise addition of amine was avoided as an impractical route for NMR monitoring purposes. Immediately upon the addition of amine, a color change was observed, and then the reaction mixture was stirred for a few minutes and an aliquot was taken via a syringe and transferred into an NMR tube along with CDCl_3 added through a septum.

Scheme 7. Potential Connection of Amine Catalytic Cycle and the Formation of an Isolated Imine–Boron Complex 21

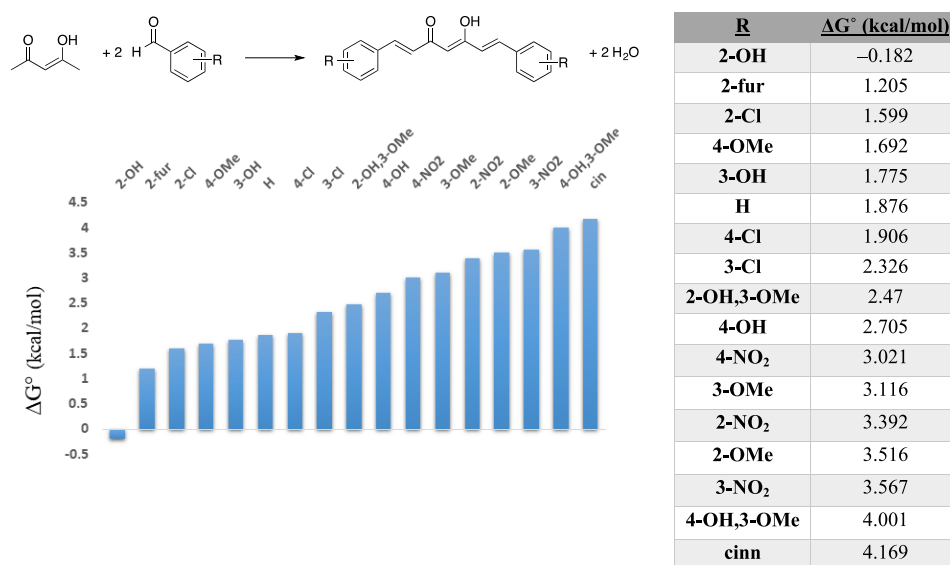
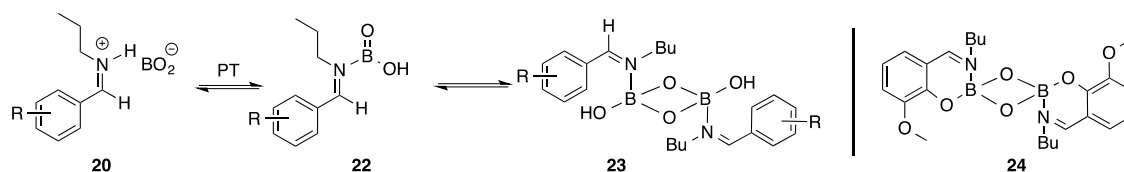


Figure 8. Modeled change in free energy (ΔG°) for the formation of a variety of curcuminoids synthesized from acetylacetone. Values provided by the rank of lowest to greatest ΔG° .

The data clearly demonstrate that upon the addition of the amine, the reaction occurs at the aldehyde and not at the sidearm of intermediate 5. The two signals appear to broaden with a second addition of amine, with an aldehyde signal still present but in a lower quantity (Figure 6b). Upon the third addition, a further change occurs, and the third signal appears in the aldehyde range, indicating the potential formation of another intermediate (Figure 6c). As the reaction progresses after the last addition of amine, the signal of aldehyde disappears and only two intermediate signals remain in the mixture (Figure 6d). It is important to note that throughout the first 45 min of the reaction, no signals belonging to the bridging or enolic hydrogens $[-C(=O)CH=C(OH)-]$ or trans-coupling signals were observed in the full spectra despite the blood-red color of the reaction mixture. Further monitoring of the reaction at approximately 1 h illustrated the initiation of condensation between the unknown activated intermediates and complex 5 due to the appearance of signals of trans-coupling bridge hydrogens.

In an attempt to isolate intermediates observed on the NMR scale, the reactions were interrupted at different times by quenching with water and ethyl acetate mixtures. When using vanillin, desired results were not achieved, and in most cases, they produced the starting aldehyde, boric acid, and curcumin product. It is interesting to note that although the reactions were interrupted in the early stages of product formation, no appreciable amounts of monoaddition product were isolated along with curcumin. The obtained quenched reaction mixtures were separated using vacuum filtration. The solid products were subjected to crystallization using a variety of solvents. The best results were obtained using dichloro-

methane as it allowed for a quick separation of large amounts of boric acid prior to recrystallization of the remaining reaction components. For reactions carried out with *ortho*-vanillin, the imine–boron complex 21 (Figure 7) was isolated, providing support for the formation of an iminium intermediate for the first time, and its cocrystal with CH_2Cl_2 was crystallographically characterized. The compound was crystallographically characterized as a cocrystal 21·0.94 CH_2Cl_2 and unambiguously confirmed the formation of a bond between the nitrogen and carbon atoms of the aldehyde. This indicates that the nucleophilic attack on the aldehyde (Scheme 6, step c) is potentially preceded by the formation of imine in the reaction mixture.

The formation of compound 21 can be accomplished through a series of steps (Scheme 7) starting with aldiminium intermediate 20 that was previously introduced in Figure 5 as a part of the alternative catalytic role of the amine. Although compounds 20 and 21 can exist as *cis* or *trans* isomers, it is arguably not essential to include both to illustrate the path (Scheme 7). The generic aldiminium intermediate can undergo a proton transfer to form the neutral compound 22 in which nitrogen is bound to boron. Dimerization of complex 22 would provide the bridged product 23 where the nitrogen is still part of the imine component, but the boron portions are now shared between the two imine fragments. The suggested pathway also provides insight as to why a similar intermediate could not be isolated for reactions of vanillin as was for *ortho*-vanillin; the close proximity of a hydroxy group to the boron center allows for the additional stabilization and the formation of intermediates 21 and 24, which is not possible for most aldehydes lacking an *ortho*-OH group. These results could also

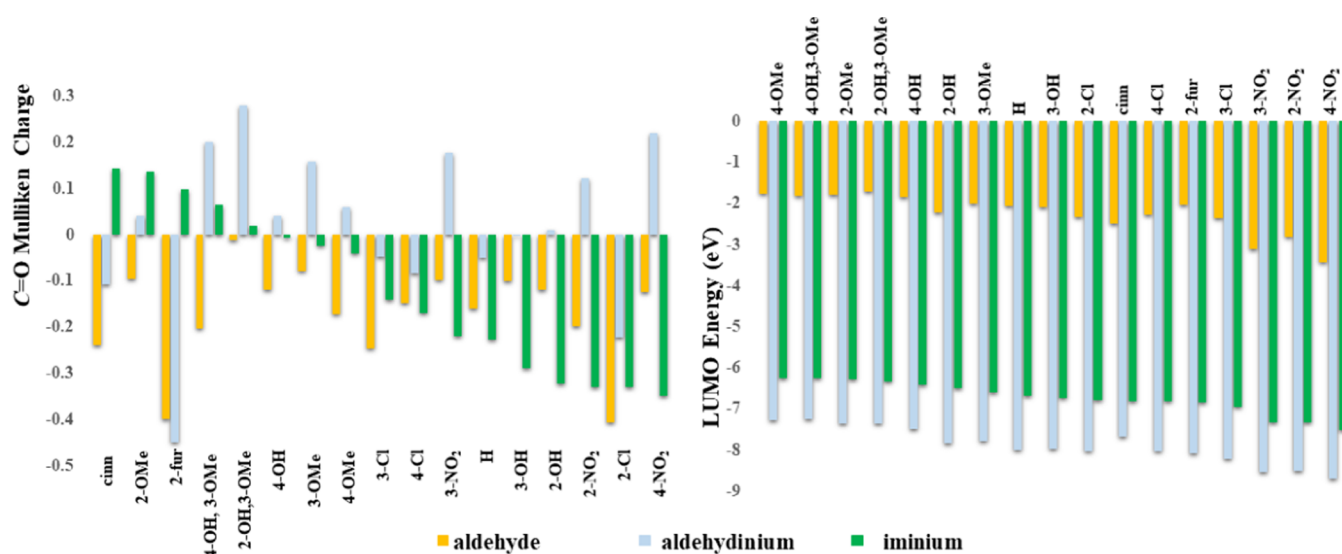


Figure 9. Mulliken charges of carbonyl carbons (left) and LUMO energies (right, in eV) for suggested target electrophiles in curcumin synthesis. Mulliken charge values provided by the rank of the most positive to most negative (left to right) iminium ions. LUMO energies provided by the rank of highest to lowest (left to right) for iminium ions.

offer a potential explanation for the aforementioned low performance of *ortho*-hydroxybenzaldehyde; however, attempts to isolate a similar intermediate from reaction mixtures with other aldehydes were not successful.

COMPUTATIONAL RESULTS AND DISCUSSION

Correlation of Free Energy and Experimental Results.

A wide range of yields have been reported in conjunction with the variety of substituent variations employed both in the literature^{5,7,8,10} and in this work. Despite the frequency with which this is encountered and reported, little if any explanation has been put forward—quite likely, this fact is tied to an incomplete picture of the mechanistic pathway of this reaction.

Several computational approaches were undertaken to attempt to explain or, at minimum, find a correlation with observations of specific, experimentally challenging targets. The first simple analysis has been to model the free-energy change from the essential reaction components and exclude all else (neglecting solvent, B-containing components, and amine). This effort was an attempt to ascertain basic thermodynamic comparisons across a range of substituents. The impact of the relative positioning and patterns across either or both of substitutional positions and substituent electronic effects was studied (Figure 8).

Due to the inconclusive trends, a full mechanistic investigation of this reaction was undertaken. Given the complexity of these reaction systems, the electronic properties of the aldehyde precursors (Figure 9) were studied first. These appeared as a reasonable comparison point, considering that this is the only point of variation structurally, and thus synthetically, that could give rise to the observed wide range of yields and the stark discrepancies in the ease of isolation. Mulliken charges of the carbonyl carbon (presuming that a nucleophilic attack step at the said spot is an initial, key mechanistic step) as well as LUMO energies were compared for an array of precursor aldehydes.

Isolated yields and the modeled substituent effects of aldehydes did not correlate. This could be due to the conversion of aldehyde in the key mechanistic step into an iminium ion. To investigate ethyl amine, the electronics of the

experimentally used *n*-butyl amine was mimicked due to fewer conformational isomers. The protonated aldehydes, aldehydes, and related *N*-ethyliminium ions were modeled. The protonated aldehydes are unlikely to be present in significant quantities due to the basic reaction conditions (Scheme 6).

The energies of the LUMOs (Figure 9) of the iminium ion (depicted in green) and to a lesser extent aldehydinium ions (depicted in blue), as compared to aldehydes, more strongly correlate to the observed product yields. Given the low likelihood of a protonated aldehyde under common reaction conditions, the iminium ion seems the most plausible electrophile target. Previously, a few reports have detailed successes under acidic reaction conditions, some of which lack an amine altogether, which could be explained by computational results (Figure 9).

An additional parameter for all three possible targets (aldehyde, aldehydinium, and iminium), the electrophilicity index (ω) was calculated (Figure 10). Electrophilicity index is

$$\omega = \frac{\mu^2}{2\eta}, \text{ where } \mu = \frac{1}{2}(E_{\text{HOMO}} + E_{\text{LUMO}}), \eta = -\frac{1}{2}(E_{\text{HOMO}} - E_{\text{LUMO}})$$

Figure 10. Formula for the calculation of electrophilicity index (ω) from chemical potential (μ) and chemical hardness (η).

a measure of a molecule's ability to accept electrons and is derived from the values of chemical potential (μ) and chemical hardness, η (Figure 11).^{27–30} The values for these species as a whole (i.e., aldehydes versus the alternatives) clearly indicate the significantly lower electrophilicity of aldehydes, another indicator of the likely lesser role in the mechanism. The aldehydinium and iminium produce a roughly similar ranking, with a couple of notable exceptions.

All structures from the previously proposed catalytic cycle (Figure 5) were modeled to ascertain the plausibility of the cycle on a step-by-step basis. As shown in Figure 12, all steps are energetically accessible, especially under the presumed heating conditions. Surprisingly, protonation of the aldehyde (−2.68 kcal/mol) is quite favorable as is the subsequent formation of the iminium ion (+0.50 kcal/mol). Also

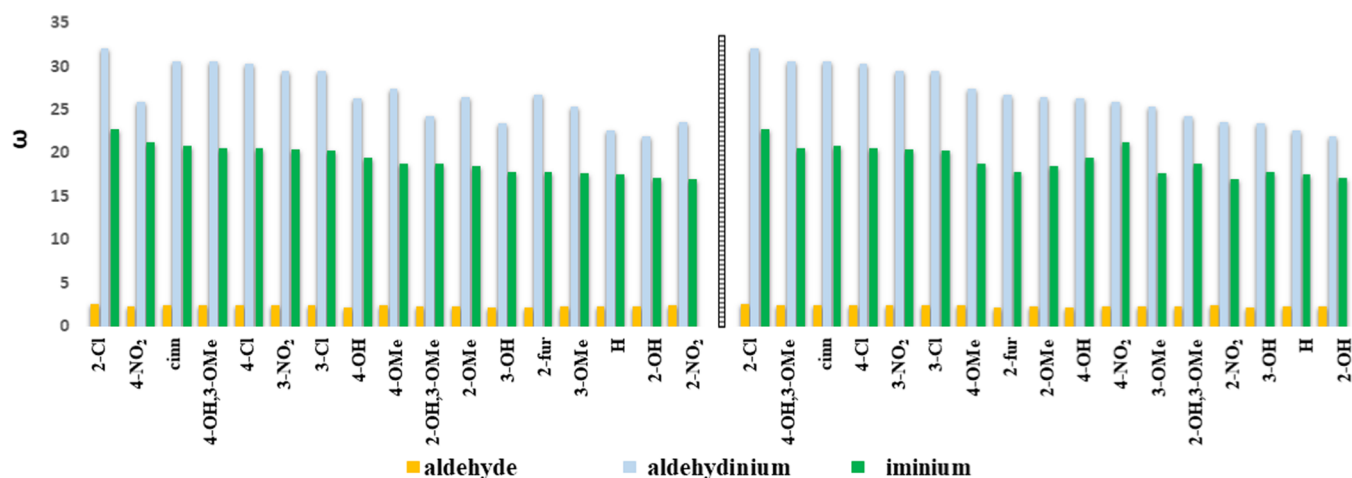


Figure 11. Calculated electrophilicity indices (ω) for suggested target electrophiles in the ranking order of iminium ions (left) and aldehydinium ions (right).

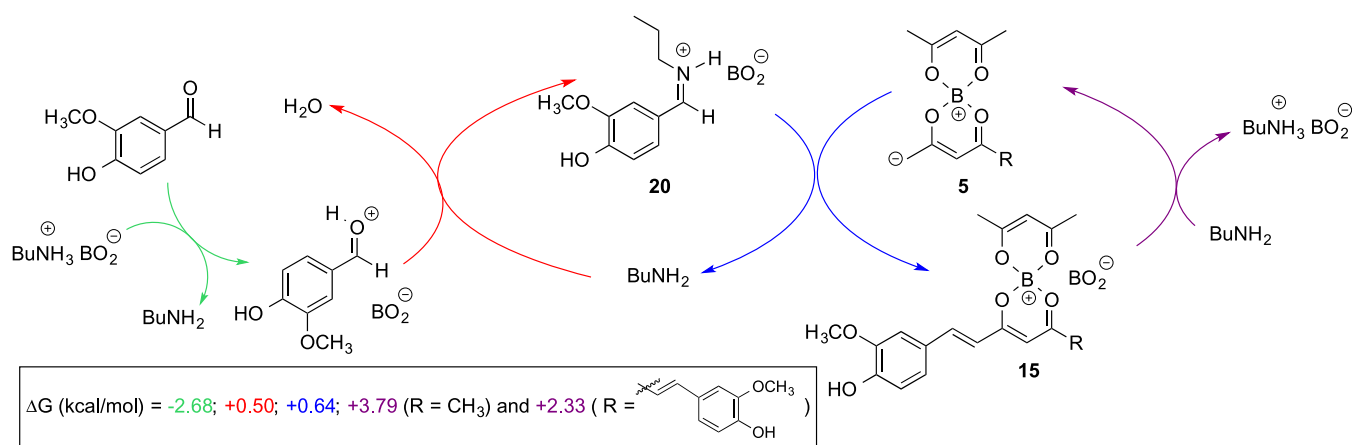


Figure 12. Net free energies (in kcal/mol) for each step of the proposed catalytic cycle.

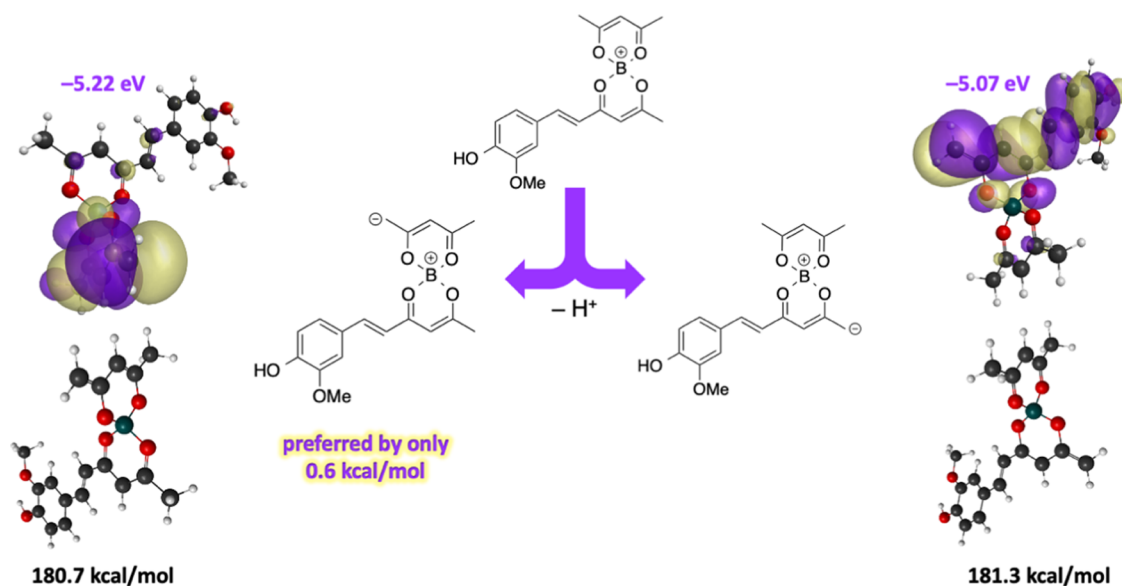


Figure 13. Optimized isomeric structures for deprotonated positions on the boron-coordinated monocondensation product. HOMOs for both isomers clearly indicate the isolation of electron lone pair to one ligand only. Molecular orbitals depicted with a contour value of 0.015.

noteworthy is the lower-energy requirement for the deprotonation of the ligated monoaddition (+2.33 kcal/mol) product

versus acac itself (+3.79 kcal/mol). This could correlate to experimental difficulties in obtaining monoaddition products

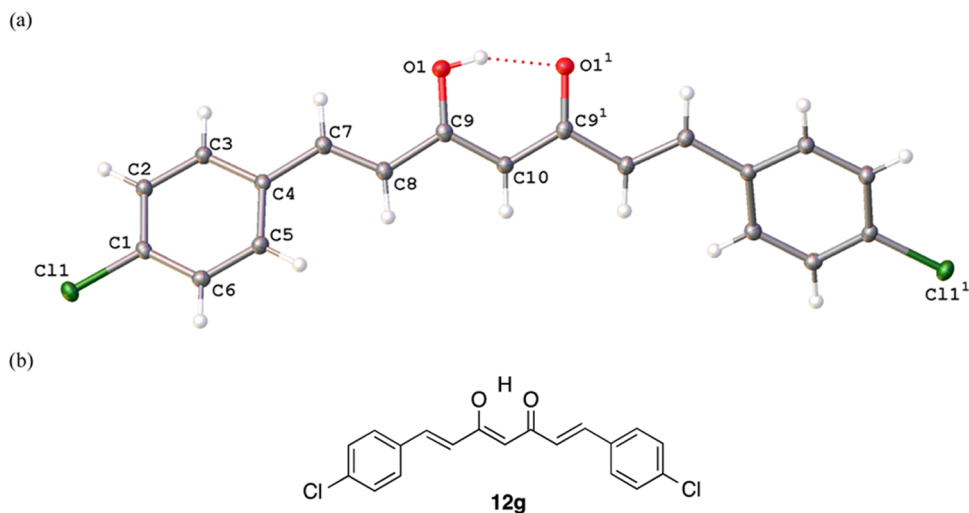


Figure 14. (a) Molecular drawing of **12g** shown with 50% probability ellipsoids. Symmetry code: (i) $-x, 1 - y, z$, and (b) its chemical structure.

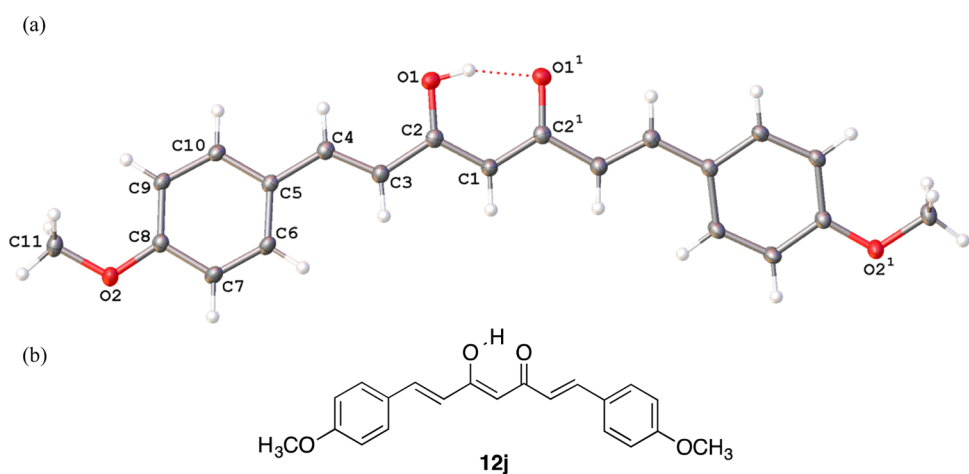


Figure 15. (a) Molecular drawing of compound **12j** shown with 50% probability ellipsoids [symmetry code: (i) $1 - x, y, 3/2 - z$] and (b) its chemical structure.

even when the unreacted aldehyde is present in conjunction with a diaddition curcuminoid product.

A few approaches have been reported provided to producing asymmetric curcuminoids using the central acetylacetonate unit as the linker.³¹ These approaches are drawn-out, multistep procedures. These routes are necessary as it is common knowledge among those that synthesize curcumin and related curcuminoids that the synthesis of asymmetrically substituted curcuminoids or, alternatively monocondensation products of acetylacetonate, is not feasible via simple stoichiometric control alone. A key initiating step for subsequent condensations is the deprotonation of the boron complex containing a mono-addition product (resulting from the first addition of aldehyde) as well as the unaltered acetylacetonate moiety (Figure 13). Not surprisingly, the two possible deprotonation products (from the two distinct β -diketonate ligands) are nearly equivalent in energy, differing by only 0.62 kcal/mol.

Crystallographic Study of Isolated Compounds.

Curcuminoids usually appear as colored powders and are often purified by recrystallization. Yet, obtaining high-quality single crystals of these compounds suitable for structural analysis is often difficult. As of today, a few crystal structures of curcuminoid-containing aromatic rings and acetylacetonate or 2-

acetylacetonate as a central linker are known, considering numerous examples of compounds synthesized. Curcumin **1** has been structurally characterized at several temperatures.³² A total of only nine structural reports exist for curcuminoids contained within this paper: *o*-OMe **12h** (CCDC 841100),³³ *p*-OH **12m** (CCDC 1117584, 1163657, 1867868–1867871),³⁴ *p*-OMe **12j** (CCDC 1486216),³⁵ and the unsubstituted aryl ring **12a** (CCDC 1123476).³⁶ These structures all contain the curcuminoid in the enol form. This includes the structure of **12j** previously reported as the keto form that could arguably be reinterpreted as being in the enol form.

Single-crystal X-ray diffraction analysis of compound **12g** ($R=4\text{-Cl}$) reveals that in the solid state the molecule exists as an enolic tautomer (Figure 14). The stereochemistries at the double bonds were conclusively established as E; the enolic double bond showed the expected Z geometry due to the six-membered cyclic transition state between the two enolic forms involving a hydrogen-bonding interaction between the carbonyl group and the enolic hydroxyl functionality. The O–H \cdots O interaction is characterized by a donor–acceptor distance of 2.514(2) Å and an OHO angle of 158(4)°. This correlates with the ¹H NMR spectrum where a peak ($\delta \sim 17$ ppm

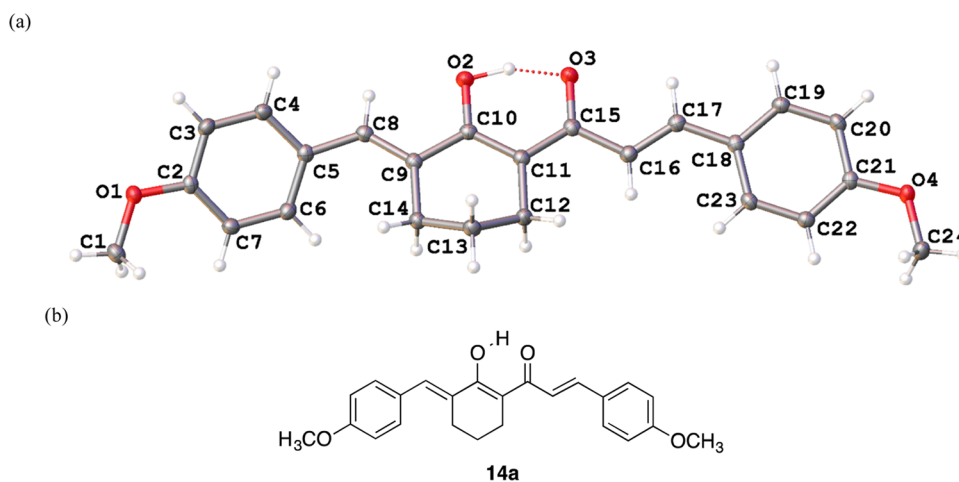


Figure 16. (a) Molecular drawing of compound **14a** shown with 50% probability ellipsoids and (b) its chemical structure.

downfield to TMS) for the chelated hydroxyl group was observed.

Similarly, in the solid-state, compound **12j** ($R=4\text{-OCH}_3$) exists as an enolic tautomer with an *E*-geometry of double bonds and the enolic double bond in the *Z* geometry (Figure 15). This result complements the previous report of a keto form for the same compound (CCDC 1486216).³⁵ The six-membered cyclic transition state between the two enolic forms involves an $\text{O-H}\cdots\text{O}$ hydrogen-bonding interaction with a donor–acceptor distance of 2.5048(15) and an OHO angle of 159(3)°. This correlates with the ¹H NMR spectrum where a peak ($\delta \sim 16$ ppm downfield to TMS) for the chelated hydroxyl group was observed.

A single-crystal diffraction study of compound **14a** ($R=4\text{-OMe}$) was undertaken to unambiguously establish the geometries about the double bond (Figure 16). These are difficult to ascertain by NMR for two of the three alkene bonds of which one is enolic. In the solid state, the molecule exists as two enolic tautomers. The stereochemistries at the exocyclic and cinnamoyl double bonds were conclusively established as *E*; the enolic double bond showed the expected *Z* geometry due to the six-membered cyclic transition state between the two enolic forms involving a hydrogen-bonding interaction between the carbonyl group and the enolic hydroxyl functionality. The $\text{O-H}\cdots\text{O}$ interaction is characterized by a donor–acceptor distance of 2.4433(10) Å and an OHO angle of 158.0(19)°. This correlates with the ¹H NMR data where a peak ($\delta \sim 17$ ppm downfield to TMS) for the chelated hydroxyl group was observed.

Study of Polymorphism of Isolated Compounds.

Polymorphism, multiple inequivalent solid-state forms of a single compound, is a well-known phenomenon. Physical properties, including, but not limited to, solubility and melting point (two pharmaceutically important physical properties) can vary, sometimes widely, for related polymorphs. The polymorphism of curcumin specifically has been well studied,^{37–40} and, furthermore, the effect of polymorphism on the melting point of curcumin has been clearly described.³⁷ The range of workup procedures (e.g., columns, solvents, temperatures, etc.) and the variance in the practices of recrystallization have quite likely led to multiple polymorphic forms all being reported as a single compound. While technically correct, this could serve as an explanation for the wide range in reported melting points for some curcuminoids.

To the best of our knowledge, there have been no efforts reported on the investigation of polymorphism of curcuminoids.⁴⁰

The reported melting points were summarized, with full details and references provided in the Supporting Information. These data demonstrate the potential importance of polymorphism for this class of compounds and could increase the awareness of a wider community of the interpretation of results from synthetic characterization and biological studies for curcuminoids. Curcumin **1**, despite being the most studied and well known, is no exception. In summary, across literature reports, melting points of curcumin **1** vary from 168 to 185 °C. Even listings of commercial sources for curcumin across multiple vendors and suppliers vary from 170 to 188 °C.⁴¹ For other curcuminoids, literature reports show even wider variance in melting points—the most extreme examples being **12a** (118–145 °C, across 12 reports), **12j** (136–168 °C, across 14 reports), **12m** (147–250 °C, across 18 reports), and **13c** (134–214 °C, across 8 reports). Considering the role of melting as a common means of purity determination and, in some cases, a quick route to product confirmation, this disparity in reported melting points could be leading to the use of product mixtures, more so than individual compounds, for some of the myriad reported biological activity tests.

CONCLUSIONS

A series of curcuminoids were obtained by an improved solvent-free, synthetic approach. All compounds were obtained, with yields that meet or exceed those observed for solvent-based methods. The main advantages of the applied method are versatility, reduced hazardous waste, and simplified isolation of products. Comprehensive assessment of correlation between structural features, reaction conditions, and product yield demonstrated that electron-enriched aldehydes provided higher yields when compared to electron-poor aldehydes regardless of the attachment point. Prolonged reaction times and increased temperatures had a relatively small impact on the overall yields. Two crystal structures were obtained for symmetric and asymmetric curcuminoids with *p*-methoxybenzyl substituents. Computational analyses further support the generalized observation that substituent type and attachment point are poor-predictive indicators of yield outcomes for a preparatory method. Mechanistic investigations support the proposed iminium ion formation as a preceding step to the

nucleophilic attachment at the aryl aldehyde carbon. An intermediate was isolated and structurally characterized. The combined experimental and computational data provide valuable insights for further investigations of the mechanism and limitations of curcuminoid synthesis.

EXPERIMENTAL SECTION

General Methods. All commercially available reagents were purchased from Millipore Sigma-Aldrich and used without further purification; all deuterated solvents were stored with molecular sieves when appropriate. Melting points were measured using a DigiMelt and are uncorrected. NMR spectra (^1H) were collected using a Bruker Avance III NMR spectrometer and were measured at 400 and 125 MHz, respectively, with $\text{DMSO-}d_6$, CDCl_3 , and CD_3OD or their combinations as the solvent. $^{11}\text{B}\{^1\text{H}\}$ and ^{11}B NMR spectra were acquired on a JEOL ECX-300 NMR spectrometer. Boron spectra were measured at 96 MHz and referenced to external 15% $\text{BF}_3\cdot\text{OEt}_2$ in CDCl_3 ($\delta = 0$ ppm). The chemical shifts (δ) are reported in parts per million relative to the residual deuterated solvent signal or external standard, as appropriate, and coupling constants (J) are given in Hertz. Elemental analyses were obtained using external sources, MidWest Microlabs LLC and/or Atlantic Microlab Inc.

ESA-TOF MS Analysis. The mass spectrometric analyses were performed using the high-resolution time-of-flight G1969A with atmospheric pressure chemical ionization (Agilent, Santa Clara, CA). The samples (10 ppm) were introduced to the MS using direct infusion at a flow rate of 100 $\mu\text{L}/\text{min}$. For analysis, samples were dissolved in 50% methanol in water. The positive ionization was performed at a voltage of 3000–5000 V and with a fragmentor set to 150–250 V with a corona needle (2–10 μA). The nitrogen was used as nebulizing (30 psig) and drying (5 L/min) gases at a temperature of 350 $^\circ\text{C}$ and heat vaporizer temperature to 350 $^\circ\text{C}$. The analysis was performed in the mass range of 100–1000 m/z . The mass spectra are shown as obtained and following blank correction (50% methanol).

Computational Methods. All structures were modeled at the B3LYP⁴²/6-311++G**⁴³ level of theory using the computational chemistry suite, GAMESS (2019 R2).⁴⁴ Implicit solvent modeling was employed for all structures using the conductor-like polarizable continuum model (C-PCM). All structures were modeled in the solvent CHCl_3 . Preoptimization was completed using Avogadro.⁴⁵ All modeled structures and orbital renderings were completed using wxMacMolPlt.⁴⁶ All structures were verified as true minima, as indicated by the absence of imaginary vibrational frequencies.

Mechanistic Studies. For the investigation of boron intermediates, a reaction was set up as described in the general procedure. A sample of the neat reaction mixture (~20 mg) was taken out after the addition of acetylacetone, aldehyde, butyl borate, and amine for NMR analysis. For investigation of the amine role, a reaction was set up as described in the general procedure without the addition of amine. A sample (~20 mg) was taken out through a septum prior to each subsequent addition of amine. For the isolation of intermediates, reactions were set up as described above. A sample (~20 mg) was taken to confirm product formation followed by quenching reactions with water. Extraction followed by crystallization produced crystals suitable for analysis, which were obtained using the DCM/EtOH mixture at room temperature using slow evaporation or vapor diffusion with hexane methods.

General Procedure for Solvent-Free Synthesis of Curcumin(oids). Boric anhydride (0.1250 g, 1.800 mmol) was combined with acetylacetone (257 mL, 2.50 mmol). The formed white paste was gently stirred for up to 10 min in a capped vial. Tri(*n*-butyl) borate (2.70 mL, 10.05 mmol) was then added via micropipette followed by the addition of vanillin (0.7608 g, 5.000 mmol). After initial stirring, to the combined mixture, *n*-butyl amine was added (12.5 mL, 0.1266 mmol) in four portions within a 10 min interval via a syringe. The reaction mixture generally would change color at the first addition of catalyst. The vial was capped using a septum and a fitted drying tube. The reaction was carried out at the specified temperatures and times.

General Procedure for Isolation of Curcumin(oids). To the reaction vial, a 50:50 mixture of ethyl acetate and DI water was added in small portions while stirring. With the separation of the reaction mixture into layers, slow precipitation of the product would proceed over the course of 30–45 min. An increase in precipitation time would typically result in a substantial increase in viscosity and subsequently hinder product separation. If necessary, the addition of EtOAc and/or water was repeated to ensure the removal of *n*-butanol from the interface of layers based on individual reactions. Decanting of the solvent mixture was followed by vacuum filtration. After washing with DI water to remove the residual, boric acid impurity would yield the desired product. Overnight drying in vacuum oven at elevated temperature allowed the removal of residual amounts of water and butanol yielding pure samples as colored powders. Melting points and NMR data are in agreement with those previously reported (see the Supporting Information for details).

ASSOCIATED CONTENT

Supporting Information

The Supporting Information is available free of charge at <https://pubs.acs.org/doi/10.1021/acsomega.1c07006>.

FAIR data include the primary NMR FID files for compounds: 12a–c, 12f, 12g, 12j, 12m, 13a–d, and 14a (ZIP)

Crystallographic data for 2051020 (21) (CIF)

Crystallographic data for 2051021 (14a) (CIF)

Crystallographic data for 2051022 (12j) (CIF)

Crystallographic data for 2051023 (12g) (CIF)

Melting point literature data comparison (Table S1); characterization of compounds, images of ^1H NMR spectra, and ^1H NMR (CDCl_3) spectrum of compound 12a and expansions (Figure S1); ^1H NMR (CDCl_3) spectrum of compound 12b and expansions (Figure S2); ^1H NMR (CDCl_3) spectrum of compound 12c and expansions (Figure S3); ^1H NMR (CDCl_3) spectrum of compound 12f and expansions (Figure S4); ^1H NMR (CDCl_3) spectrum of compound 12g and expansions (Figure S5); ^1H NMR ($\text{DMSO-}d_6$) spectrum of compound 12j and expansions (Figure S6); ^1H NMR ($\text{DMSO-}d_6$) spectrum of compound 12m and expansions (Figure S7); ^1H NMR (CDCl_3) spectrum of compound 13a and expansions (Figure S8); ^1H NMR (CDCl_3) spectrum of compound 13b and expansions (Figure S9); ^1H NMR (CDCl_3) spectrum of compound 13c and expansions (Figure S10); ^1H NMR (CDCl_3) spectrum of compound 13d and expansions (Figure S11); ^1H NMR (CDCl_3) spectrum of compound 14a

and expansions (Figure S12); crystallographic data tables (Table S2); modeling data and electronic structure parameters of aldehydes, aldehydinium ions, and *N*-ethyliminium ions (Table S3); modeled aldehydes (Scheme S1); atomic coordinates for aldehydes (Table S4); modeled protonated aldehydes (Scheme S2); atomic coordinates for protonated aldehydes (Table S5); modeled *N*-ethyliminium ions (Scheme S3); atomic coordinates for *N*-ethyliminium ions (Table S6); atomic coordinates for modeled curcuminoids (Table S7); modeled free energies for substances in the proposed catalytic cycle in Figure 12 (Table S8); atomic coordinates for substances modeled in the proposed catalytic cycle in Figure 12 (Table S9); and references (PDF)

Accession Codes

CCDC 2051020 (21), 2051021 (14a), 2051022 (12j), and 2051023 (12g) contain the supplementary crystallographic data for this paper. These data can be obtained free of charge via www.ccdc.cam.ac.uk/data_request/cif, or by emailing data_request@ccdc.cam.ac.uk, or by contacting The Cambridge Crystallographic Data Centre, 12 Union Road, Cambridge CB2 1EZ, U.K.; fax: +44 1223 336033.

AUTHOR INFORMATION

Corresponding Author

Valeria A. Stepanova – Department of Chemistry and Biochemistry, University of Wisconsin La Crosse, La Crosse, Wisconsin 54601, United States; orcid.org/0000-0001-6026-513X; Email: vstepanova@uwlax.edu

Authors

Andres Guerrero – Department of Chemistry and Biochemistry, University of Wisconsin La Crosse, La Crosse, Wisconsin 54601, United States

Cullen Schull – Department of Chemistry and Biochemistry, University of Wisconsin La Crosse, La Crosse, Wisconsin 54601, United States

Joshua Christensen – Department of Chemistry and Biochemistry, University of Wisconsin La Crosse, La Crosse, Wisconsin 54601, United States

Claire Trudeau – Department of Chemistry and Biochemistry, University of Wisconsin La Crosse, La Crosse, Wisconsin 54601, United States

Joshua Cook – Department of Chemistry and Biochemistry, University of Wisconsin La Crosse, La Crosse, Wisconsin 54601, United States

Kyle Wolmuth – Department of Chemistry and Biochemistry, University of Wisconsin La Crosse, La Crosse, Wisconsin 54601, United States

Jordan Blochwitz – Department of Chemistry and Biochemistry, University of Wisconsin La Crosse, La Crosse, Wisconsin 54601, United States

Abdelrahman Ismail – Department of Chemistry and Biochemistry, University of Wisconsin La Crosse, La Crosse, Wisconsin 54601, United States

Joseph K. West – Department of Chemistry, Winona State University, Winona, Minnesota 55987, United States; orcid.org/0000-0003-0021-9638

Amelia M. Wheaton – Department of Chemistry, University of Wisconsin-Madison, Madison, Wisconsin 53706, United States

Ilia A. Guzei – Department of Chemistry, University of Wisconsin-Madison, Madison, Wisconsin 53706, United States; orcid.org/0000-0003-1976-7386

Bin Yao – Department of Chemistry, University of North Dakota, Grand Forks, North Dakota 58202, United States

Alena Kubatova – Department of Chemistry, University of North Dakota, Grand Forks, North Dakota 58202, United States; orcid.org/0000-0002-2318-5883

Complete contact information is available at: <https://pubs.acs.org/10.1021/acsomega.1c07006>

Author Contributions

[†]A.G. and C.S. contributed equally to this work.

Notes

The authors declare no competing financial interest.

ACKNOWLEDGMENTS

The authors acknowledge the Minnesota Supercomputing Institute (MSI) at the University of Minnesota for providing resources that contributed to the research results reported within this paper. URL: <http://www.msi.umn.edu>. The authors acknowledge the Department of Chemistry at Winona State University for the access to their JEOL ECX-300 NMR spectrometer to collect research results reported within this paper. The instrument was funded by NSF Award #DUE-0126470 in 2001. The authors acknowledge the Molecular Structure Laboratory at the University of Wisconsin–Madison for providing resources that contributed to the research results reported within this paper. The Bruker D8 VENTURE Photon III X-ray diffractometer was partially funded by NSF Award #CHE-1919350 to the UW–Madison Department of Chemistry. The Bruker Quazar APEX2 was purchased by the UW–Madison Department of Chemistry with a portion of a generous gift from Paul J. and Margaret M. Bender. The authors acknowledge the Department of Chemistry at UW–La Crosse for the access to the Bruker Avance III 400 NMR spectrometer to collect research results reported within this paper. The instrument was funded by NSF Award #CHE-0923388 in 2009. The authors acknowledge UW–La Crosse McNair Program, Dean's office of the College of Science and Health, and the Hardy W. Chan and Sons Summer Undergraduate Research Fellowship (SURF) for the generous financial support provided to undergraduate research students that contributed to the research results reported within this paper: Guerrero (McNair Scholar 2018), Schull (Dean's Distinguished Summer Fellowship 2020), and Christensen (Hardy W. Chan & Sons 2017 SURF). The authors also acknowledge financial support from the UW–La Crosse Undergraduate Research and Creativity (URC) office.

REFERENCES

- (1) (a) Esatbeyoglu, T.; Huebbe, P.; Ernst, I. M.; Chin, D.; Wagner, A. E.; Rimbach, G. Curcumin—from Molecule to Biological Function. *Angew. Chem., Int. Ed.* **2012**, *51*, 5308–5332. (b) Priyadarsini, K. I. The Chemistry of Curcumin: from Extraction to Therapeutic Agent. *Molecules* **2014**, *19*, 20091–20112. (c) Kocaadam, B.; Şanlıer, N. Curcumin, an Active Component of Turmeric (*Curcuma longa*), and Its Effects on Health. *Crit. Rev. Food Sci. Nutr.* **2017**, *57*, 2889–2895. (d) Agarwal, S.; Mishra, R.; Gupta, A. K.; Gupta, A. Turmeric: Isolation and Synthesis of Important Biological Molecules. In *Synthesis of Medicinal Agents from Plants*; Elsevier Ltd., 2018. (e) Meng, F.; Zhou, Y.; Ren, D.; Wang, R. et al. Turmeric: A Review of Its Chemical Composition, Quality Control, Bioactivity, and

- Pharmaceutical Application. In *Handbook of Food Bioengineering, Natural and Artificial Flavoring Agents and Food Dyes*; Academic Press, 2018.
- (2) (a) Chattopadhyay, K.; Biswas, U.; Bandyopadhyay, R. K.; Banerjee, I. Turmeric and Curcumin: Biological Actions and Medicinal Applications. *Curr. Sci.* **2004**, *87*, 44–53. (b) Menon, V. P.; Sudheer, A. R. Antioxidant and Anti-Inflammatory Properties of Curcumin. *Adv. Exp. Med. Biol.* **2007**, *595*, 105–125. (c) Agrawal, D. K.; Mishra, P. K. Curcumin and Its Analogues: Potential Anticancer Agents. *Med. Res. Rev.* **2010**, *30*, 818–860. (d) Fan, X.; Zhang, C.; Liu, D. B.; Yan, J.; Liang, H. P. The Clinical Applications of Curcumin: Current State and the Future. *Curr. Pharm. Des.* **2013**, *19*, 2011–2031. (e) Yang, Z.; Zhao, T.; Zhang, J. H.; Feng, H.; et al. Curcumin Inhibits Microglia Inflammation and Confers Neuroprotection in Intracerebral Hemorrhage. *Immunol. Lett.* **2014**, *160*, 89–95. (f) Oliveira, A. S.; Sousa, E.; Vasconcelos, M. H.; Pinto, M. Curcumin: a Natural Lead for Potential New Drug Candidates. *Curr. Med. Chem.* **2015**, *22*, 4196–4232. (g) Nelson, K. M.; Dahlin, J. L.; Bisson, J.; Graham, J.; Pauli, G. F.; Walters, M. A. The Essential Medicinal Chemistry of Curcumin. *J. Med. Chem.* **2017**, *60*, 1620–1637. (h) Ramayanti, O.; Brinkkemper, M.; Verkuijlen, S. A. W. M.; Rittmaleni, L.; Go, M. L.; Middeldorp, J. M. Curcuminoids as EBV Lytic Activators for Adjuvant Treatment in EBV-Positive Carcinomas. *Cancers* **2018**, *10*, 89–108.
- (3) (a) Grand View Research. *Global Curcumin Market 2019 by Manufacturers, Regions, Type and Application, Forecast to 2024*; Report identifier: GIR-13875731; 2019. <https://www.industryresearch.biz/global-curcumin-market-13875731>. (b) Market Analysis Report. *Curcumin Market Size, Share & Trends Analysis Report by Application (Pharmaceutical, Food, Cosmetics), by Region (North America, Europe, Asia Pacific, Central & South America, Middle East & Africa), and Segment Forecasts, 2020–2027*; Report identifier: 978-1-68038-431-4; 2020. <https://www.grandviewresearch.com/industry-analysis/turmeric-extract-curcumin-market>.
- (4) Roughley, P. J.; Whiting, D. A. Experiments in the Biosynthesis of Curcumin. *J. Chem. Soc., Perkin Trans. 1* **1973**, 2379–2388.
- (5) (a) Masuda, T.; Jitoe, A.; Isobe, J.; Nakatani, N.; Yonemori, S. Anti-oxidative and Anti-inflammatory Curcumin-Related Phenolics from Rhizomes of Curcuma Domestica. *Phytochemistry* **1993**, *32*, 1557–1560. (b) Nurfina, A.; Reksahadiprodjo, M. S.; Timmerman, H.; Jenie, U. A.; Sugiyanto, D.; van der Goot, H. Synthesis of Some Symmetrical Curcumin Derivatives and Their Antiinflammatory Activity. *Eur. J. Med. Chem.* **1997**, *32*, 321–328. (c) Ferrari, E.; Lazzari, S.; Marverti, G.; Pignedoli, F.; Spagnolo, F.; Saladini, M. Synthesis, Cytotoxic and Combined cDDP Activity of New Stable Curcumin Derivatives. *Bioorg. Med. Chem.* **2009**, *17*, 3043–3052. (d) Khan, M. A.; El-Khatib, R.; Rainsford, K. D.; Whitehouse, M. W. Synthesis and Anti-inflammatory Properties of Some Aromatic and Heterocyclic Aromatic Curcuminoids. *Bioorg. Chem.* **2012**, *40*, 30–38. (e) Yin, S.; Zheng, X.; Yao, X.; Wang, Y.; Liao, D. Synthesis and Anticancer Activity of Mono-Carbonyl Analogues of Curcumin. *J. Cancer Ther.* **2013**, *04*, 113–123. (f) Fang, L.; Gou, S.; Liu, X.; Cao, F.; Cheng, L. Design, Synthesis and Anti-Alzheimer Properties of Dimethylaminomethylsubstituted Curcumin Derivatives. *Bioorg. Med. Chem. Lett.* **2014**, *24*, 40–43. (g) Zou, P.; Zhang, J.; Xia, Y.; Kanchana, K.; Guo, G.; Chen, W.; Huang, Y.; Wang, Z.; Yang, S.; Liang, G. ROS Generation Mediates the Anti-Cancer Effects of WZ35 via Activating JNK and ER Stress Apoptotic Pathways in Gastric Cancer. *Oncotarget* **2015**, *6*, 5860–5876. (h) Aluwi, M. F. F. M.; Rullah, K.; Yamin, B. M.; Leong, S. W.; Bahari, A. M. N.; Lim, S. J.; Faudzi, M. S. M.; Jalil, J.; Abas, F.; Fauzi, N. M.; Ismail, N. H.; Jantan, I.; Lam, K. W. Synthesis of Unsymmetrical Monocarbonyl Curcumin Analogues with Potent Inhibition on Prostaglandin E2 Production in LPS-induced Murine and Human Macrophages Cell Lines. *Bioorg. Med. Chem. Lett.* **2016**, *26*, 2531–2538.
- (6) (a) Zhang, Y.; Zhao, L.; Wu, J.; Jiang, X.; Dong, L.; Xu, F.; Zou, P.; Dai, Y.; Shan, X.; Yang, S.; Liang, G. Synthesis and Evaluation of a Series of Novel Asymmetrical Curcumin Analogs for the Treatment of Inflammation. *Molecules* **2014**, *19*, 7287–7307. (b) Singh, H.; Kumar, M.; Nepali, K.; Gupta, M. K.; Saxena, A. K.; Sharma, S.; Bedi, P. M. S. Triazole Tethered C5-Curcuminoid-Coumarin Based Molecular Hybrids as Novel Antitubulin Agents: Design, Synthesis, Biological Investigation and Docking Studies. *Eur. J. Med. Chem.* **2016**, *116*, 102–115. (c) Wiji Prasetyaningrum, P.; Bahtiar, A.; Hayun, H. Synthesis and Cytotoxicity Evaluation of Novel Asymmetrical Mono-Carbonyl Analogues of Curcumin (AMACs) Against Vero, HeLa, and MCF7 Cell Lines. *Sci. Pharm.* **2018**, *86*, No. 25. (d) Rodrigues, F. C.; Kumar, A. N. V. A.; Thakur, G. Developments in the Anticancer Activity of Structurally Modified Curcumin: an Up-To-Date Review. *Eur. J. Med. Chem.* **2019**, *177*, 76–104. (e) Nouredin, S. A.; El-Shishtawy, R. M.; Al-Footy, K. O. Curcumin Analogues and Their Hybrid Molecules as Multifunctional Drugs. *Eur. J. Med. Chem.* **2019**, *182*, 111631–111671.
- (7) Khor, P. Y.; Aluwi, M. F. F. M.; Rullah, K.; Lam, K. W. Insights on the Synthesis of Asymmetric Curcumin Derivatives and Their Biological Activities. *Eur. J. Med. Chem.* **2019**, *183*, 111704–111725.
- (8) Pabon, H. J. A Synthesis of Curcumin and Related Compounds. *Recl. Trav. Chim. Pays-Bas* **1964**, *83*, 379–386.
- (9) (a) Miłobędzka, J.; Kostanecki, S. V.; Lampe, V. Structure of curcumin. *Ber. Dtsch. Chem. Ges.* **1910**, *43*, 2163–2170. (b) Pavolini, T.; Cumberbar, F.; Crinzuto, A. M. Curcumin and curcuminoids. *Ann. Chim. Roma* **1950**, *40*, 280–287.
- (10) Krakov, M. H.; Edward, B. H. Process for the Synthesis of Curcumin-Related Compounds. U.S. Patent US5,679,864, 1997.
- (11) (a) Kulkarni, P. S.; Kondhare, D. D.; Ravi, V.; Zubaidha, P. K. Calcium Hydroxide: an Efficient and Mild Base for One-Pot Synthesis of Curcumin and Its Analogues. *Acta Chim. Slovaca* **2013**, *6*, 150–156. (b) Shioorkar, M. G.; Ubale, M. B.; Jadhav, S. A.; Pardeshi, R. K. Simple and Effective Microwave Assisted One Pot Synthesis of Symmetrical Curcumin Analogues. *Chem. Sin.* **2015**, *6*, 110–113.
- (12) Spicer, G. S.; Strickland, J. D. H. Compounds of Curcumin and Boric Acid. Part I. The Structure of Rosocyanin. Part II. The Structure of Rubrocurcumin. Part III. Infra-red Studies of Rosocyanin and Allied Compounds. *J. Chem. Soc.* **1952**, 4644–4650.
- (13) John, J.; Rugmini, S. D.; Nair, B. S. Kinetics and Mechanism of the Thermal and Hydrolytic Decomposition Reaction of Rosocyanin. *Int. J. Chem. Kinet.* **2018**, *50*, 164–177.
- (14) Chopra, A. K.; Moss, G. P.; Weedon, B. C. L. Carotenoids and Related Compounds. Part 40. Synthesis of Triketoriorhodin and Other p-Diketones. *J. Chem. Soc., Perkin Trans. 1* **1988**, 1371–1382.
- (15) Arrieta, A. Direct synthesis of demethoxycurcumin. *C. R. Acad. Sci. Ser. II* **1994**, *318*, 479–482.
- (16) Mullins, J. J.; Prusinowski, A. F. Microwave-Promoted Synthesis of a Carbocyclic Curcuminoid: an Organic Chemistry Laboratory Experiment. *J. Chem. Educ.* **2019**, *96*, 606–609.
- (17) (a) Smoliakova, I. P.; Wood, J. L.; Stepanova, V. A.; Mawo, R. Y. Solvent-free Cyclopalladation on Silica Gel. *J. Organomet. Chem.* **2010**, *695*, 360–364. (b) Stepanova, V. A.; Kukowski, J. E.; Smoliakova, I. P. Cyclopalladation of 2-Tert-butyl-4,4-dimethyl-2-oxazoline in Solution and on Silica gel. *Inorg. Chem. Commun.* **2010**, *13*, 653–655. (c) Stepanova, V. A.; Egan, L. M.; Stahl, L.; Smoliakova, I. P. Reactions of Benzylidiphenylphosphine with Pd(II) Sources on Silica Gel. *J. Organomet. Chem.* **2011**, *696*, 3162–3168. (d) Kukowski, J. E.; Lamb, J. R.; Stepanova, V. A.; Smoliakova, I. P. Solvent-free Direct Cyclopalladation of Sulfides on Silica Gel. *Inorg. Chem. Commun.* **2012**, *26*, 64–65. (e) Lamb, J. R.; Stepanova, V. A.; Smoliakova, I. P. Transcyclopalladation on silica gel. *Polyhedron* **2013**, *53*, 202–207.
- (18) Pore, D.; Alli, R.; Prabhakar, A. S. C.; Alavala, R. R.; Kulandaivelu, U.; Boyapati, S. Solid-Phase Microwave Assisted Synthesis of Curcumin Analogs. *Lett. Org. Chem.* **2012**, *9*, 447–450.
- (19) (a) Wang, J.; Zhang, X.; Yan, J.; Li, W.; Jiang, Q.; Wang, X.; Zhao, D.; Cheng, M. Design, Synthesis and Biological Evaluation of Curcumin Analogues as Novel LSD1 Inhibitors. *Bioorg. Med. Chem. Lett.* **2019**, *29*, 126683. (b) Baikerikar, S. Curcumin and Natural Derivatives Inhibit Ebola Viral Proteins: An in Silico Approach. *Pharmacogn. Res.* **2017**, *9*, 15–22. (c) Wongrattanakamon, P.; Ampasavate, D.; Sirithunyalug, B.; Jiranusomkul, S. An Integrated

- Molecular Modeling Approach for the Tryptase Monomer-Curcuminoid Recognition Analysis: Conformational and Bioenergetic Features. *J. Bioenerg. Biomembr.* **2018**, *50*, 447–459. (d) Orteca, G.; Tavanti, F.; Bednarikova, Z.; Gazova, Z.; Rigillo, G.; Imbriano, C.; Basile, V.; Asti, M.; Rigamonti, L.; Saladini, M.; Ferrari, E.; Menziani, M. C. Curcumin Derivatives and $\alpha\beta$ -fibrillar Aggregates: An Interactions' Study for Diagnostic/Therapeutic Purposes in Neurodegenerative Diseases. *Bioorg. Med. Chem.* **2018**, *26*, 4288–4300. (e) Laali, K. K.; Greves, W. J.; Correa-Smits, S. J.; Zwarycz, A. T.; Bunge, S. D.; Borosky, G. L.; Manna, A.; Paulus, A.; Chanan-Khan, A. Novel Fluorinated Curcuminoids and Their Pyrazole and Isoxazole Derivatives: Synthesis, Structural Studies, Computational/Docking and *In-vitro* Bioassay. *J. Fluorine Chem.* **2018**, *206*, 82–98. (f) Suent-Santiago, V.; Moraes, J.; de, B. B.; Alves, E. S. S.; Vannier-Santos, M. A.; Freire-de-Lima, C. G.; Castro, R. N.; Mandes-Silva, G. P.; de Nigris Del Cistia, C.; Magalhaes, L. G.; Andricopulo, A. D.; Sant Anna, C. M. R.; Decote-Ricardo, D.; Friere de Lima, M. E. The Effectiveness of Natural Diarylheptanoids Against *Trypanosoma cruzi*: Cytotoxicity, Ultrastructural Alterations and Molecular Modeling Studies. *PLoS One* **2016**, *11*, No. e0162926. (g) Randino, R.; Grimaldi, M.; Persico, M.; De Santis, A.; Cini, E.; Cabri, W.; Riva, A.; D'Errico, G.; Fattorusso, C.; D'Urso, A. M.; Rodriguez, M. Investigating the Neuroprotective Effects of Turmeric Extract: Structural Interactions of β -Amyloid Peptide with Single Curcuminoids. *Sci. Rep.* **2016**, *6*, No. 33846.
- (20) (a) Insuasty, D.; Cabrera, L.; Ortiz, A.; Insuasty, B.; Quiroga, J.; Abonia, R. Synthesis, Photophysical Properties and Theoretical Studies of New Bis-quinolin Curcuminoid BF₂-Complexes and Their Decomplexed Derivatives. *Spectrochim. Acta, Part A* **2020**, *230*, 118065. (b) Raikwar, M. M.; Rhyman, L.; Ramasami, P.; Sekar, N. Theoretical Investigation of Difluoroboron Complex of Curcuminoid Derivatives with and without Phenyl Substituent (at Meso Position): Linear and Non-linear Optical Study. *ChemistrySelect* **2018**, *3*, 11339–11349. (c) Etcheverry-Berrios, A.; Olavarria, I.; Perrin, M. L.; Diaz-Torres, R.; Julian, D.; Ponce, I.; Zagal, J. H.; Pavez, J.; Vasquez, S. O.; van der Zant, H. S. J.; Dulic, D.; Aliaga-Alcade, N.; Soler, M. Multiscale Approach to the Study of the Electronic Properties of Two Thiophene Curcuminoid Molecules. *Chem. - Eur. J.* **2016**, *22*, 12808–12818. (d) Margar, S. N.; Sekar, N. Nonlinear Optical Properties of Curcumin: Solvatochromism-based Approach and Computational Study. *Mol. Phys.* **2016**, *114*, 1867–1879. (e) Srivastava, S.; Gupta, P.; Sethi, A.; Singh, R. P. One Pot Synthesis of Curcumin-NSAIDs Prodrug, Spectroscopic Characterization, Conformational Analysis, Chemical Reactivity, Intramolecular Interactions and First-order Hyperpolarizability by DFT Method. *J. Mol. Struct.* **2016**, *1117*, 173–180. (f) Alsalim, T. A. A. Q.; Saeed, B. A.; Elias, R. S.; Abbo, H. S.; Titinchi, S. J. Synthesis and Electronic Properties of Alkyl- and Alkoxy-Curcuminoids. *Eur. J. Chem.* **2013**, *4*, 70–73.
- (21) (a) Hazarika, R.; Kalita, B. Elucidating the Therapeutic Activity of Selective Curcumin Analogues: DFT-based Reactivity Analysis. *Struct. Chem.* **2021**, *32*, 1701–1715. (b) Nag, A.; Chakraborty, P.; Natarajan, G.; Baksi, A.; Mudedla, S. K.; Subramanian, V.; Pradeep, T. Bent Keto Form of Curcumin, Preferential Stabilization of Enol by Piperine, and Isomers of Curcumin/Cyclodextrin Complexes: Insights from Ion Mobility Mass Spectrometry. *Anal. Chem.* **2018**, *90*, 8776–8784. (c) Santin, L. G.; Toledo, E. M.; Carvalho-Silva, V. H.; Camargo, A. J.; Gargano, R.; Oliveira, S. S. Methanol Solvation Effect on the Proton Rearrangement of Curcumin's Enol Forms: An *Ab Initio* Molecular Dynamics and Electronic Structure Viewpoint. *J. Phys. Chem. C* **2016**, *120*, 19923–19931. (d) Kong, X.; Brinkmann, A.; Terskikh, V.; Wasylishen, R. E.; Bernard, G. M.; Duan, Z.; Wu, Q.; Wu, G. Proton Probability Distribution in the O•••H•••O Low-barrier Hydrogen Bond: A Combined Solid-state NMR and Quantum Chemical Computational Study of Dibenzoylmethane and Curcumin. *J. Phys. Chem. B* **2016**, *120*, 11692–11704. (e) Agnihotri, N.; Mishra, P. C. Scavenging Mechanism of Curcumin Toward the Hydroxyl Radical: A Theoretical Study of Reactions Producing Ferulic Acid and Vanillin. *J. Phys. Chem. A* **2011**, *115*, 14221–14232. (f) Kolev, T. M.; Velcheva, E. A.; Stamboliyska, B. A.; Spittler, M. DFT and Experimental Studies of the Structure and Vibrational Spectra of Curcumin. *Int. J. Quantum Chem.* **2005**, *102*, 1069–1079.
- (22) Babu, K. V.; Rajasekharan, K. N. Simplified Condition for Synthesis of Curcumin and Other Curcuminoids. *Org. Prep. Proced. Int.* **1994**, *26*, 674–677.
- (23) Rao, E. V.; Sudheer, P. Revisiting Curcumin Chemistry Part I: a New Strategy for the Synthesis of Curcuminoids. *Indian J. Pharm. Sci.* **2011**, *73*, 262–270.
- (24) Liu, K.; Chen, J.; Chojnacki, J.; Zhang, S. BF₃·OEt₂-Promoted Concise Synthesis of Difluoroboron-Derivatized Curcumins from Aldehydes and 2,4-Pentanedione. *Tetrahedron Lett.* **2013**, *54*, 2070–2073.
- (25) Weiss, H.; Reichel, J.; Goris, H.; Schneider, K. R. A.; Micheel, M.; Prohl, M.; Gottschaldt, M.; Dietzek, B.; Weigand, W. Curcuminoid-BF₂ Complexes: Synthesis, Fluorescence and Optimization of BF₂ Group Cleavage. *Beilstein J. Org. Chem.* **2017**, *13*, 2264–2272.
- (26) Carmona-Vargas, C. C.; Alves, L. C.; Brocksoma, T. J.; de Oliveira, K. T. Combining Batch and Continuous Flow Setups in the End-to-End Synthesis of Naturally Occurring Curcuminoids. *React. Chem. Eng.* **2017**, *2*, 366–374.
- (27) (a) Mehrani, S.; Tayyari, S. F.; Heravi, M. M.; Morsali, A. Theoretical Investigation of Solvent Effect on the Keto-Enol Tautomerization of Pentane-2,4-dione and a Comparison Between Experimental and Theoretical Calculations. *Can. J. Chem.* **2021**, *99*, 411–424. (b) Adeniyi, A. A.; Conradie, J. Influence of Substituents on the Reduction Potential and pK_a values of β -diketones Tautomers: A Theoretical Study. *Electrochim. Acta* **2019**, *297*, 947–960. (c) Dutta, A.; Boruah, B.; Saikia, P. M.; Dutta, R. K. Stabilization of Diketo Tautomer of Curcumin by Perfluorinated Cationic Surfactants: A Spectroscopic, Tensiometric and TD-DFT Study. *J. Mol. Liq.* **2013**, *187*, 350–358. (d) Raissi, H.; Yoosefian, M.; Hajizadeh, A.; Imampour, J. S.; Karimi, M.; Farzad, F. Theoretical Description of Substituent Effects in 2,4-Pentanedione: AIM, NBO, and NMR Study. *Bull. Chem. Soc. Jpn.* **2012**, *85*, 87–92.
- (28) Parr, R. G.; Pearson, R. G. Absolute Hardness: Companion to Absolute Electronegativity. *J. Am. Chem. Soc.* **1983**, *105*, 7512–7516.
- (29) Parr, R. G.; Szentpaly, L.; Liu, S. Electrophilicity Index. *J. Am. Chem. Soc.* **1999**, *121*, 1922–1924.
- (30) Chattaraj, P. K.; Roy, D. R. Update 1 of: Electrophilicity Index. *Chem. Rev.* **2007**, *107*, PR46–PR47.
- (31) (a) Sundaryono, A.; Nourmamode, A.; Gardrat, C.; Frtisch, A.; Castellano, A. Synthesis and Complexation Properties of Two New Curcuminoid Molecules Bearing a Diphenylmethane Linkage. *J. Mol. Struct.* **2003**, *649*, 177–190. (b) Shao, W.-Y.; Cao, Y.-N.; Yu, Z.-W.; Pan, W.-J.; Qiu, X.; Bu, X.-Z.; An, L.-K.; Huang, Z.-S.; Gu, L.-Q.; Chan, A. S. C. Facile Preparation of New Unsymmetrical Curcumin Derivatives by Solid-phase Synthesis Strategy. *Tetrahedron Lett.* **2006**, *47*, 4085–4089.
- (32) Groom, C. R.; Bruno, I. J.; Lightfoot, M. P.; Ward, S. C. The Cambridge Structural Database. *Acta Crystallogr., Sect. B: Struct. Sci., Cryst. Eng. Mater.* **2016**, *72*, 171–179.
- (33) Zhao, Y.-L.; Groundwater, P. W.; Hibbs, D. E.; Nguyen, P. K.; Narlawar, R. (1E,4Z,6E)-5-Hydroxy-1,2-bis(2-methoxyphenyl)-1,4,6-heptatrien-3-one. *Acta Crystallogr., Sect. E: Struct. Rep. Online* **2011**, *67*, o1885.
- (34) (a) Tønnesen, H. H.; Karlsen, J.; Mostad, A.; Pedersen, U.; Rasmussen, P. B.; Lawesson, S.-O.; et al. Structural Studies of Curcuminoids. II. Crystal Structure of 1,7-Bis(4-hydroxyphenyl)-1,6-heptadiene-3,5-dione Methanol Complex. *Acta Chem. Scand.* **1983**, *37b*, 179–185. (b) Karlsen, J.; Mostad, A.; Tonnesen, H. H.; et al. Structural Studies of Curcuminoids. VI. Crystal Structure of 1,7-Bis(4-hydroxyphenyl)-1,6-heptadiene-3,5-dione Hydrate. *Acta Chem. Scand.* **1988**, *42b*, 23–27. (c) Yuan, L.; Horosanskaia, E.; Engelhardt, F.; Edelmann, F. T.; Couvrat, N.; Sanselme, M.; Cartigny, Y.; Coquerel, G.; Seidel-Morgenstern, A.; Lorenz, H. Solvate Formation of Bis(dimethoxy)curcumin: Crystal Structure Analyses and Stability Investigations. *Cryst. Growth Des.* **2019**, *19*, 854–857.

(35) Azizi, K.; Esfandiary, N.; Karimi, M.; Kazemi, M.; Heydari, A. Direct Oxidative Esterification of Toluene with 1,3-Dicarbonyl Compounds Catalyzed by Copper Complex Supported on Magnetic Nanoparticles. *Appl. Organomet. Chem.* **2017**, *31*, No. e3658.

(36) Mostad, A.; Pedersen, U.; Rasmussen, P. B.; Lawesson, S.-O. Structural Studies of Curcuminoids. III. Crystal Structure of 1,7-Diphenyl-1,5-heptadiene-3,5-dione. *Acta Chem. Scand.* **1983**, *37b*, 901–905.

(37) Sanphui, P.; Goud, N. R.; Khandavilli, U. B. R.; Bhanoth, S.; Nangia, A. New Polymorphs of Curcumin. *Chem. Commun.* **2011**, *47*, 5013–5015.

(38) Mishra, M. K.; Sanphui, P.; Ramamurty, U.; Desiraju, G. R. Solubility-Hardness Correlation in Molecular Crystals: Curcumin and Sulfathiazole Polymorphs. *Cryst. Growth Des.* **2014**, *14*, 3054–3061.

(39) Matlinska, M. A.; Wasylshen, R. E.; Bernard, G. M.; Terskikh, V. V.; Brinkmann, A.; Michaelis, V. K. Capturing Elusive Polymorphs of Curcumin: A Structural Characterization and Computational Study. *Cryst. Growth Des.* **2018**, *18*, 5556–5563.

(40) Dai, Y.; Terskikh, V.; Brinkmann, A.; Wu, G. Solid-State ¹H, ¹³C, and ¹⁷O NMR Characterization of the Two Uncommon Polymorphs of Curcumin. *Cryst. Growth Des.* **2020**, *20*, 7484–7491.

(41) Sigma-Aldrich: C1386, C7727, 78246, 8.20354. Acros Organics: C/8850/43. TCI America: C2302. All accessed June 29, 2021.

(42) (a) Becke, A. D. Density-Functional Thermochemistry. III. The Role of Exact Exchange. *J. Chem. Phys.* **1993**, *98*, 5648–5652. (b) Lee, C.; Yang, W.; Parr, R. G. Development of the Colle-Salvetti Correlation-Energy Formula into a Functional of the Electron Density. *Phys. Rev. B* **1988**, *37*, 785–789. (c) Vosko, S. H.; Wilk, L.; Nusair, M. Accurate Spin-Dependent Electron Liquid Correlation Energies for Local Spin Density Calculations: a Critical Analysis. *Can. J. Phys.* **1980**, *58*, 1200–1211. (d) Stephens, P. J.; Devlin, F. J.; Chabalowski, C. F.; Frisch, M. J. Ab Initio Calculation of Vibrational Absorption and Circular Dichroism Spectra Using Density Functional Force Fields. *J. Phys. Chem. A* **1994**, *98*, 11623–11627.

(43) (a) Clark, T.; Chandrasekhar, J.; Spitznagel, G. W.; Schleyer, P. V. R. Efficient Diffuse Function-Augmented Basis Sets for Anion Calculations. III. The 3-21+G Basis Set for First-Row Elements, Li-F. *J. Comput. Chem.* **1983**, *4*, 294–301. (b) Francl, M. M.; Pietro, W. J.; Hehre, W. J.; Binkley, J. S.; Gordon, M. S.; DeFrees, D. J.; Pople, J. A. Self-Consistent Molecular Orbital Methods. XXIII. A Polarization-Type Basis Set for Second-Row Elements. *J. Chem. Phys.* **1982**, *77*, 3654–3665. (c) Krishnan, R.; Binkley, J. S.; Seeger, R.; Pople, J. A. Self-Consistent Molecular Orbital Methods. XX. A Basis Set for Correlated Wave Functions. *J. Chem. Phys.* **1980**, *72*, 650–654. (d) McLean, A. D.; Chandler, G. S. Contracted Gaussian Basis Sets for Molecular Calculations. I. Second Row Atoms, Z=11-18. *J. Chem. Phys.* **1980**, *72*, 5639–5648. (e) Spitznagel, G. W.; Clark, T.; Schleyer, P. V. R.; Hehre, W. J. An Evaluation of the Performance of Diffuse Function-Augmented Basis Sets for Second Row Elements, Na-Cl. *J. Comput. Chem.* **1987**, *8*, 1109–1116.

(44) Barca, G. M. J.; Bertoni, C.; Carrington, L.; Datta, D.; De Silva, N.; Deustua, J. E.; Fedorov, D. G.; Gour, J. R.; Gunina, A. O.; Guidez, E.; Harville, T.; Irle, S.; Ivancic, J.; Kowalski, K.; Leang, S. S.; Li, H.; Li, W.; Lutz, J. J.; Magoulas, I.; Mato, J.; Mironov, V.; Nakata, H.; Pham, B. Q.; Piecuch, P.; Poole, D.; Pruitt, S. R.; Rendell, A. P.; Roskop, L. B.; Ruedenberg, K.; Sattasathuchana, T.; Schmidt, M. W.; Shen, J.; Slipchenko, L.; Sosonkina, M.; Sundriyal, V.; Tiwari, A.; Vallejo, J. L. G.; Westheimer, B.; Wloch, M.; Xu, P.; Zahariev, F.; Gordon, M. S. Recent Developments in the General Atomic and Molecular Electronic Structure System. *J. Chem. Phys.* **2020**, *152*, 154102.

(45) (a) Avogadro: An Open-Source Molecular Builder and Visualization Tool, Version 1.2.0. <http://avogadro.cc/>. (b) Hanwell, M. D.; Curtis, D. E.; Lonie, D. C.; Vandermeersch, T.; Zurek, E.; Hutchison, G. R. Avogadro: An advanced semantic chemical editor, visualization, and analysis platform. *J. Cheminf.* **2012**, *4*, No. 17.

(46) Bode, B. M.; Gordon, M. S. MacMolPlt: a Graphical User Interface for GAMESS. *J. Mol. Graphics Modell.* **1998**, *16*, 133–138.